(12) INTERNATIONAL APPLICATION PUBLISHED UNDER THE PATENT COOPERATION TREATY (PCT)

(19) World Intellectual Property Organization
International Bureau

(43) International Publication Date
17 May 2018 (17.05.2018)

WIPO | PCT

(10) International Publication Number
WO 2018/089553 A1

(51) International Patent Classification:
C12N 5/00 (2006.01) *C12N 5/0735* (2010.01)
C12N 5/02 (2006.01) *C12N 5/075* (2010.01)
C12N 5/073 (2010.01) *C12N 5/16* (2006.01)

(21) International Application Number:
PCT/US2017/060720

(22) International Filing Date:
08 November 2017 (08.11.2017)

(25) Filing Language: English

(26) Publication Language: English

(30) Priority Data:
62/419,638 09 November 2016 (09.11.2016) US
62/427,546 29 November 2016 (29.11.2016) US

(71) Applicant: **OREGON HEALTH & SCIENCE UNIVERSITY** [US/US]; Office of Technology Transfer & Business Development, 0690 SW Bancroft Street, Portland, OR 97239-3098 (US).

(72) Inventors; and
(71) Applicants: **MITALIPOV, Shoukhrat** [US/US]; Oregon Health & Sciences University, 0690 SW Bancroft Street, Portland, OR 97239 (US). **GUIERREZ, Nuria, Marti** [US/US]; Oregon Health & Sciences University, 0690 SW Bancroft Street, Portland, OR 97239 (US). **TEMIAKOV, Dmitry** [US/US]; Oregon Health & Sciences University, 0690 SW Bancroft Street, Portland, OR 97239 (US).

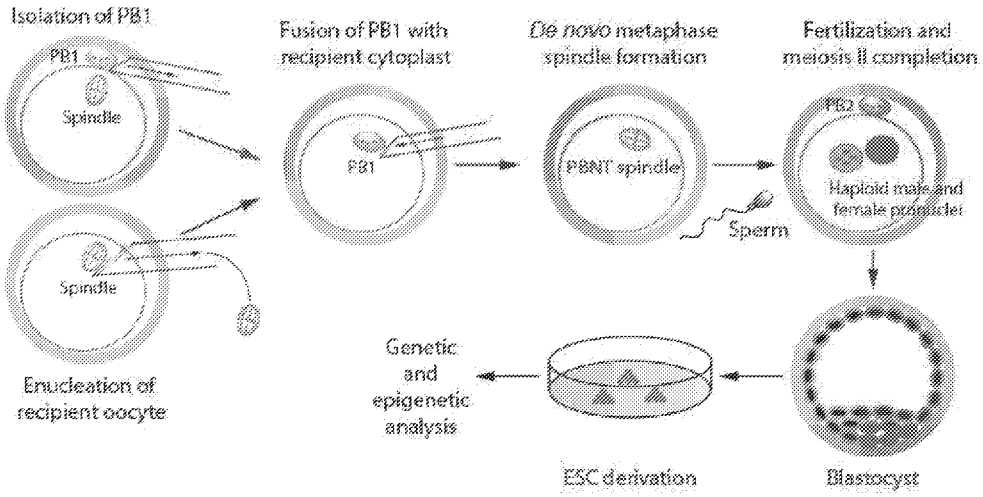
(74) Agent: **ECK, Steven, R.**; Office of Technology Transfer & Business Development, Oregon Health & Sciences University, 0690 SW Bancroft Street, Portland, OR 97239 (US).

(81) Designated States *(unless otherwise indicated, for every kind of national protection available)*: AE, AG, AL, AM, AO, AT, AU, AZ, BA, BB, BG, BH, BN, BR, BW, BY, BZ, CA, CH, CL, CN, CO, CR, CU, CZ, DE, DJ, DK, DM, DO, DZ, EC, EE, EG, ES, FI, GB, GD, GE, GH, GM, GT, HN, HR, HU, ID, IL, IN, IR, IS, JO, JP, KE, KG, KH, KN, KP, KR, KW, KZ, LA, LC, LK, LR, LS, LU, LY, MA, MD, ME, MG, MK, MN, MW, MX, MY, MZ, NA, NG, NI, NO, NZ, OM, PA, PE, PG, PH, PL, PT, QA, RO, RS, RU, RW, SA, SC, SD, SE, SG, SK, SL, SM, ST, SV, SY, TH, TJ, TM, TN, TR, TT, TZ, UA, UG, US, UZ, VC, VN, ZA, ZM, ZW.

(84) Designated States *(unless otherwise indicated, for every kind of regional protection available)*: ARIPO (BW, GH, GM, KE, LR, LS, MW, MZ, NA, RW, SD, SL, ST, SZ, TZ, UG, ZM, ZW), Eurasian (AM, AZ, BY, KG, KZ, RU, TJ, TM), European (AL, AT, BE, BG, CH, CY, CZ, DE, DK, EE, ES, FI, FR, GB, GR, HR, HU, IE, IS, IT, LT, LU, LV, MC, MK, MT, NL, NO, PL, PT, RO, RS, SE, SI, SK, SM, TR), OAPI (BF, BJ, CF, CG, CI, CM, GA, GN, GQ, GW, KM, ML, MR, NE, SN, TD, TG).

(54) Title: GENERATION OF HUMAN OOCYTES

Figure 1A



(57) Abstract: Methods are provided of generating functional human oocytes following nuclear transfer of first polar body (PB1) genomes from metaphase II (MII) oocytes into enucleated donor MII cytoplasm (PBNT) and using mitochondrial replacement techniques to circumvent mother-to-child mtDNA disease transmission.

[Continued on next page]

WO 2018/089553 A1

Published:

— *with international search report (Art. 21(3))*

— *before the expiration of the time limit for amending the claims and to be republished in the event of receipt of amendments (Rule 48.2(h))*

TITLE

GENERATION OF HUMAN OOCYTES

FIELD

Generally, the field involves the generation of human oocytes in vitro by the transfer of nuclear material. More specifically, the field involves generation of human oocytes by nuclear transfer of polar bodies into enucleated donor oocytes and/or the transfer of nuclear material from an oocyte from an oocyte containing mitochondrial DNA mutations to an oocyte lacking such mutations.

BACKGROUND

Infertility attributed to both male and female factors affects millions of families around the world and while the assisted reproductive technologies (ARTs) can circumvent many cases (Huang JY and Rosenwaks Z, *Meth Mol Biol* **1154**, 171-231 (2014); incorporated by reference herein); Leridon H, *Human Reproduction* **19**, 1548-1553 (2004); Trounson A and Mohr L, *Nature* **305**, 707-709 (1983); all of which are incorporated by reference herein), it's efficacy is particularly limited by the number and quality of oocytes that decline with advanced maternal age (Leridon 2004 *supra*). Therefore, the development of additional sources of competent oocytes, genetically related to patients is desirable.

Perhaps the ultimate approach would involve the differentiation of pluripotent stem cells into primordial germ cells (PGCs) and ultimately into mature oocytes (Daley GQ *et al*, *Science* **316**, 409-410 (2007); Handel MA *et al*, *Cell* **157**, 1257-1261 (2014); Hayashi Y *et al*, *Fertil Steril* **97**, 1250-1259 (2012); Matthews TJ *et al*, *NCHS Data Brief* 1-8 (2009); all of which are incorporated by reference herein). However, the complexity of establishing an *in vitro* system for producing functional haploid human oocytes currently limits this application (Irie N *et al*, *Cell* **160**, 253-268 (2015) and Sasaki K *et al*, *Cell Stem Cell* **17**, 178-194 (2015); both of which are incorporated by reference herein).

Maternally inherited mtDNA mutations can cause fatal or severe debilitating diseases in children (Archer SL, *N Engl J Med* 369, 2236-2251 (2013); Koopman WJ *et al*, *N Engl J Med* 366, 1132-1141 (2012); and Schon E *et al*, *Nat Rev Genet* 13, 878-890 (2012); all of which are incorporated by reference herein). Disease severity is dependent on the specific gene mutation and the ratio of pathogenic to wildtype mtDNA (heteroplasmy level) in each cell and tissue (Wallace DC & Chalkia D, *Cold Spr Harb Perspect Biol* 5, a021220 (2013); incorporated by reference herein). Pathogenic mtDNA mutations are relatively common with an estimated 778 affected children born each year in the United States (Gorman GS *et al*, *N Engl J Med* 372, 885-887 (2015); incorporated by reference herein). Currently, there is no effective cure for patients with mtDNA mutations. Therefore, mitochondrial replacement techniques (MRTs) have been developed to prevent transmission of mutant mtDNA from mothers to their children (Wolf DP *et al*, *Trends Mol Med* 21, 68-76 (2015); Wang T *et al*, *Cell* 157, 1591-1604 (2014); Tachibana M *et al*, *Nature* 493, 627-631 (2013); Craven L *et al*, *Nature* 465, 82-85 (2010); and Tachibana M *et al*, *Nature* 461, 367-372 (2009); all of which are incorporated by reference herein). Regulatory agencies in the US and UK are currently evaluating clinical applications of MRT designed to assess efficacy and safety. To date, the clinical aspects of MRT have not been studied including issues of patient eligibility, embryo development and maintenance of donor mtDNA post-MRT.

There remains a need for improved methods of assisting with fertilization, implantation, and successful pregnancies in patients with declining or otherwise incompetent oocytes.

SUMMARY

Provided herein are methods for preparing oocytes for fertilization and uterine implantation.

Disclosed herein is the *de novo* reconstruction of haploid human oocytes by recycling of PB1 genomes via nuclear transfer into donor cytoplasm (Gurdon JB, *Rambam Maimonides Med J* **6** (2015), incorporated by reference herein).

Oocyte defects lie at the heart of some forms of infertility, and could potentially be addressed therapeutically by alternative routes for oocyte formation. Disclosed herein is the generation of functional human oocytes following nuclear transfer of first polar body (PB1) genomes from metaphase II (MII) oocytes into enucleated donor MII cytoplasm (polar body nuclear transfer, PBNT). The reconstructed oocytes supported the formation of *de novo* meiotic spindles and, after fertilization with sperm, meiosis completion and formation of normal diploid zygotes. While PBNT zygotes developed to blastocysts less frequently (42%) than controls (75%), genome-wide genetic, epigenetic and transcriptional analyses of PBNT and control embryonic stem cells (ESCs) indicated comparable numbers of structural variations and markedly similar DNA methylation and transcriptome profiles. PB1 genetic material via introduction into donor cytoplasm can provide oocytes for infertility treatment or mitochondrial replacement therapy for mtDNA disease.

This method allows generating additional patient-matched oocytes for treatment infertility. By utilizing each patient MII oocyte and its PB1 (plus donor cytoplasm), patient-related oocytes/embryos can be theoretically doubled. Realistically, the development of PBNT embryos to blastocysts is lower. So one can estimate that the number of viable embryos for transfer and thus pregnancy rates can increase by 40%.

Disclosed herein is a method of generating a viable human oocyte. The method involves enucleating a first oocyte at the MII stage, thereby creating a cytoplast, isolating a polar body from a second oocyte by aspiration, and placing the polar body into the perivitelline space of the cytoplast. The method can also involve fertilizing the viable human oocyte, thereby creating an embryo. The method can further comprise implanting the embryo in a receptive uterine (endometrial) lining. Enucleating the first oocyte can be performed in a medium comprising at least 10% human tubal fluid, a buffer, and cytochalasin B using a Polarized Microscope Imaging System. Isolating the polar body can be performed in a medium comprising at least 10% human tubal fluid, buffer, cytochalasin B, and fusion with the donor cytoplast can be induced with HVJ-E (hemagglutinating virus of Japan/Sendai virus envelope) extract.

Provided is a method for preparing an oocyte for fertilization, the method comprising the steps of:

a) isolating a first oocyte containing a polar body;
b) gaining access through the zona pellucida of the first oocyte;
c) removing the polar body from the first oocyte;
d) removing the nuclear spindle from a second oocyte to create an enucleated cytoplast;
e) placing the polar body removed from the first oocyte into the perivitelline space of the enucleated cytoplast.

Also provided is a method of producing a human oocyte in vitro, the method comprising:

a) determining a mitochondrial DNA sequence of the conserved sequence box II of a donor oocyte;
b) enucleating the donor oocyte while the donor oocyte is arrested at metaphase II, thereby isolating donor nuclear genetic material;
c) introducing the donor nuclear genetic material into an enucleated recipient oocyte, provided that the mitochondrial DNA of the donor oocyte has the same conserved sequence box II genotype as the recipient oocyte.

Additional embodiments of both methods above involve an additional step of fertilizing the newly created oocyte through in vitro fertilization. In additional embodiments, the fertilized oocyte/embryo is cultured to the blastocyst stage before implantation in a receptive uterus/endometrial lining.

BRIEF DESCRIPTION OF THE DRAWINGS

Color figures were submitted as part of the original disclosure and references to colors in the figures are provided in this description. Applicants reserve the right to present color versions of the figures disclosed herein in later proceedings.

Figure 1A shows the generation of haploid human oocytes by PBNT. PB1 from a donor oocyte is recovered and introduced into a recipient MII cytoplast. After fertilization, PBNT zygotes are cultured to the blastocyst stage before transfer to a patient. Alternatively, they can be used to derive embryonic stem cells for further analysis.

Figure 1B shows confocal microscopy detecting meiotic spindle-chromosomal structures in PB1 (first panel from left), intact MII (second panel) and PBNT (third-last panels) oocytes labelled with DAPI (blue) for DNA and α- and β-tubulins (green) for microtubules. Note absence of meiotic spindle apparatus in PB1 (first panel) and abnormal spindles at prophase (third panel) or anaphase (last panel) in some PBNT oocytes. Scale bars, 5 μm.

Figure 1C shows most PB1s in freshly retrieved human MII oocytes were intact with round morphology (left panel). Other MII oocytes contained fragmented or disintegrated PB1s, unsuitable for PBNT (middle and right panels). Scale bar, 100 μm.

Figure 1D shows spindle formation (arrow), detected using the Oosight™ imaging system, 60 min after PB1 was introduced into an enucleated MII cytoplast. Scale bar, 100 μm.

Figure 1E shows the completion of meiosis and pronuclear formation in human PBNT oocytes after fertilization. Note normal zygote with 2 pronuclei (2PN) and a second polar body (PB2) on left panel and abnormal 1PN, 3PN or 2PN without PB2 extrusion in other images. Scale bars, 100 μm.

Figure 1F shows a hatching blastocyst from a PBNT zygote, with prominent ICM indicated by asterisk. Scale bar, 100 μm.

Figure 1G shows a summary of fertilization and in vitro development to blastocysts of PBNT oocytes. Error bars are mean ± SEM. Significance established with Student's *t*-test. Control = intact MII oocytes.

Figure 2A shows cytogenetic G-banding analysis of PBNT1, PBNT2, and control hESO-14, hESO-15, hESO-16 and hESO-17 lines. Note, the normal female karyotypes in PBNT1 and control hESO-14 and normal male karyotypes in control hESO-16 and hESO-17. PBNT2 displayed an abnormal triploid karyotype while control hESO-15 had an abnormal karyotype with chromosome 21 monosomy.

Figure 2B shows a Venn diagram displaying the results of structural variation analysis in PBNT1, hESO-14 compared to the egg donor. PBNT1 (blue) and hESO-14 (red) had similar numbers of SVs when compared to the egg donor.

Figure 2C shows a Venn diagram displaying the results of structural variation analysis in PBNT1, hESO-14 compared to the sperm donor. PBNT1 (blue) and hESO-14 (red) had similar numbers of SVs when compared to the sperm donor.

Figure 2D shows a summary of SVs in PBNT1 and hESO-14.

Figure 3A shows the percentage of methylated CGs in PBNT1 and hESO-14 from total CG sites.

Figure 3B shows non-CG methylation rates in PBNT1 and hESO-14 among all non-CG sites.

Figure 3C shows a total of 116 CG DMRs were identified between PBNT1 and hESO-14. Genomic features of DMRs (overlap at least 1 bp) - CGI, CG islands; DHS, DNase I hypersensitivity sites, TSS, transcription start sites; TES, transcription end sites.

Figure 3D shows a representative screen shot showing one CG DMR hypomethylated in PBNT1compared to hESO-14.

Figure 3E is a set of screen shots showing four non-CG mega DMRs identified in PBNT1 compared to hESO-14.

Figure 4A is a smear plot summarizes the differential expression (DE) analysis. The log-fold change of each of the 14877 genes used in the analysis is plotted against the average abundance (log of counts-per-million) of each gene. The red dots represent the genes with significantly different expression (FDR < 0.05). The blue lines indicate 2-fold changes.

Figure 4B is a heat map showing the expression profile of the 186 DE genes. Two distinct clusters were apparent with genes expressed highly in PBNT1 cells compared to hESO-14 cells and vice versa (n = 6).

Figure 5A shows histological analyses of teratoma tumors produced after injections of PBNT1 into SCID mice. Scale bars, 100 μm. Arrows indicate neural crest-like tissues (ectoderm), cartilage-like tissues (mesoderm) and mucosal epithelium of gut-like tissues (endoderm).

Figure 5B shows histological analyses of teratoma tumors produced after injections of hESO-14 into SCID mice. Scale bars, 100 μm. Arrows indicate neural crest-like tissues (ectoderm), cartilage-like tissues (mesoderm) and mucosal epithelium of gut-like tissues (endoderm).

Figure 6A is a pedigree of Leigh Syndrome families 1 and 2.

Figure 6B is a pedigree of Leigh Syndrome G13513A family 3.

Figure 6C is a pedigree of MELAS syndrome A3243G family 5 from large pedigree (see also Figure 10B).

For all of Figures 6A, 6B, and 6C, the underlined heteroplasmy levels were obtained from previous reports. In all families, the heteroplasmy levels for mtDNA mutations were diverse among tissues and individuals, and associated with clinical disease. Black filled, diagnosed as a mitochondrial disease. LS = Leigh syndrome. y = year-old. Square = male; circle = female. B = blood; SF = skin fibroblasts; U = urine.

Figure 7A is a set of graphs showing individual oocytes harboring different heteroplasmy levels. cED = carrier oocyte donor.

Figure 7B is a set of two plots showing the average heteroplasmy level in oocytes correlated to levels in existing children rather than those in carrier oocyte donors. Heteroplasmy levels of carriers and children were measured in blood. R= Pearson's r values.

Figure 7C is a plot showing comparable mtDNA variants between oocytes with healthy mtDNA and those carrying mtDNA mutations ($p>0.05$).

Figure 7D is a plot showing that the total copy number of mtDNA was comparable in oocytes with healthy mtDNA and those carrying pathogenic mtDNA ($p>0.05$). Karyoplasts were isolated from carrier oocytes for ST except oocytes from cED2, which exhibited premature luteinization. Oocytes from healthy egg donors were mature MII. n = the number of oocytes. LS: Leigh syndrome; MELAS: mitochondrial encephalomyopathy with lactic acidosis and stroke-like episodes. t-test, ns = not significant ($p>0.05$).

Figure 8A is a set of graphs showing ST embryo development following various experimental manipulations. Similar developmental outcomes were observed among groups

except normal fertilization rate, which was significantly lower in carrier and frozen ST groups ($p<0.05$). Combinations = mixture of different mtDNA haplotypes between karyoplast and cytoplast; Intact control = non-manipulated, ICSI only.

Figure 8B is a set of graphs showing that carrier ST embryos from different mutation types showed a similar development pattern.

Figure 8C is a set of graphs showing control ST embryo development as a function of donor mtDNA matching distances. The numbers on the top of bars are percentage (%) of embryo development. N = the number of embryos. ns = not significant ($p>0.05$).

Figure 8D is a set of plots of NPCs derived from ST ESCs with 6 and 49 SNP differences in donor mtDNA displayed oxygen consumption rates (OCR) similar to non-manipulated controls. However, NPCs with 33 SNPs showed significantly reduced OCR than controls with either donor or maternal mtDNA ($p<0.05$). Seahorse assay was repeated 3 different times with 6 to 18 replicates each time. See also Figure 13A. NPCs = neural progenitor cells. SNPs = single nucleotide polymorphisms. t-test or One-way ANOVA.

Figure 9A is an image of a gel showing polymorphism in the CSBII region of donor mtDNA results in a decreased efficiency of replication primer generation by mitochondrial RNA polymerase. The 311-315CCCCC polymorphism is a shortening of the first G-stretch in the G-quadruplex region of mtDNA (G5 vs. G6 stretch), responsible for transcription termination and replication primer generation in human mitochondria.

Figure 9B is a plot showing heteroplasmy rates for the maternal mtDNA (H49 haplotype) gradually increased during *in vitro* extended culture of 3243ST-ES1 and reached homoplasmy.

Figure 9C is a plot showing that the heteroplasmy levels also increased during single ESC colony subculture.

Figure 9D is a plot showing the maintenance of stable heteroplasmy in progeny of individually cultured cells.

Figure 9E is a plot showing faster cell growth and proliferation rates in clones containing higher maternal mtDNA heteroplasmy.

Figure 9F is a set of three graphs showing maternal mtDNA heteroplasmy changes in reversed cell lines 3243ST-ES1, ST-ES7 and NT-ES8 during in vitro and in vivo differentiation. One-way ANOVA. Mean ± SD.

Figure 10A is a table showing families with mitochondrial disease and reproductive age women recruited for MRT. All LS families had an existing, severely affected child. F, family; non-syn, non-synonymous; n/a, non-applicable.

Figure 10B shows that Family 5 was selected from an extensive MELAS syndrome pedigree. Clinical phenotypes of A3243G MELAS syndrome varied even with similar heteroplasmy levels. Squares, males vs. Circles, females; B = blood and U = urine. n/t, non-tested. *, the first MELAS patient diagnosed clinically. Heteroplasmy in blood (upper) and urine (lower).

Figure 11A is a graph showing that the age of oocyte donors was similar between carrier and healthy groups.

Figure 11B is a graph showing that ovarian reserve was significantly lower in carriers relative to healthy oocyte donors.

Figure 11C is a graph showing that antral follicle count (AFC) was significantly lower in carriers relative to healthy oocyte donors.

Figure 11D is a graph showing that the duration of COS was longer in carriers.

Figure 11E is a graph showing that peak estradiol (E2) on the day of hCG trended lower in carriers.

Figure 11F is a graph showing that the total oocyte yield was significantly lower in carriers than healthy oocyte donors.

Figure 11G is a graph showing that the number of mature oocytes was significantly lower in carriers than healthy oocyte donors.

Figure 11H is a table of baseline characteristics and cycle outcomes. Carriers had higher BMI and lower AMH levels. Lower peak estradiol levels were measured in cED1 and cED2. Birth control method: combined oral contraceptive. Medroxyprogesterone.

Figure 11I is a set of two pie charts showing Analysis of heteroplasmic mtDNA variants detected in MII oocytes. *De novo* indicates unique mutations found in individual oocytes; inherited means mutations shared with other oocytes, sibling children or egg donors. n = the number of mutations in individual oocytes.

Figure 11J is a set of two plots showing that AMH levels, a measure of ovarian reserve, were not correlated with mtDNA copy number. n = the number of oocytes. ns = not significant.

Figure 12A is a table showing the results of whole mtDNA sequencing performed to identify haplotypes of all egg donors and ST was performed to match various haplotypes. Cyto, cytoplast; Karyo, karyoplast.

Figure 12B is a set of images showing normal fertilization (2PN, left) and abnormal fertilization (1 or 3 PN). See arrows.

Figure 12C is a table showing carrier ST showed higher abnormal fertilization than controls. One 3 PN zygote from control ST group developed to a blastocyst and displayed a 69, XXY karyotype. * $p<0.05$.

Figure 12D is a table showing that the blastulation rate was similar between vitrified cytoplasm with fresh spindles and vitrified spindles with fresh cytoplasm ($p>0.05$).

Figure 12E is a set of graphs showing embryo development with different donor mitochondrial DNA.

Figure 13A is a set of 15 graphs showing the results where energy metabolism (OCR/ECAR) was measured and compared between neural progenitor cells (NPCs) derived from MRT and control embryos carrying either donor or maternal mtDNA. OCR = oxygen consumption rate (representing OXPHOS), ECAR = extracellular acidification rate (representing glycolysis). NPCs from MRT ESCs with 6 and 49 SNP differences displayed comparable OCR to NPCs harboring maternal or donor mtDNA except maximal respiration in 49 SNP group. OCR was reduced in NPCs with 33 SNPs. The OCR data was normalized by live cell DNA content. *vs. host mtDNA, **vs. donor mtDNA, ***vs. ST ($p<0.05$, t-test or one-way ANOVA, n=16-18 technical replicates). Mean ± SEM.

Figure 13B is a set of graphs showing mitochondrial respiratory chain enzyme activity in differentiated cells from ST-ESCs. Mitochondrial Complex I and IV activities in differentiated cells from ST-ESCs carrying donor mtDNA with 49 SNP differences were comparable to controls with either donor or maternal mtDNA.

Figure 14A is a table showing a summary of in vitro and in vivo differentiation of ESCs derived from ST or SCNT embryos carrying donor mtDNA. Similar to control IVF-ESCs, all tested MRT ESCs produced teratoma tumors in vivo and formed neural progenitor cells (NPCs) and cardiomyocytes in vitro.

Figure 14B is a histological analysis of differentiated tissues from MRT-ESCs. The representative tissues were collected and used for mtDNA carryover analysis and measurements of mitochondrial function.

Figure 15A is a graph and table showing that the aneuploidy rate in blastocysts determined by array CGH was not significantly different in ST groups compared to control.

Figure 15B is a graph and table showing that a Karyotype abnormality rate in ESCs determined by G-banding analysis was also comparable among ST groups. Bars = mean ± s.d. Number inside bars = the number of blastocysts or ESC lines. Simple $\chi 2$ tests.

Figure 16A is a set of two plots showing maternal mtDNA (X2c haplotype) heteroplasmy increased during extended *in vitro* culture and reached homoplasmy in pooled cultures or in individual colony subcultures.

Figure 16B is a set of two graphs showing respiratory chain complex 1 (COM I) and complex 4 (COM IV) enzyme activities were measured in fibroblasts carrying various human mtDNA haplotypes used in this study. No significant differences were noted.

Figure 17 is a table summarizing array CGH in intact and ST blastocysts.

Figure 18 is a table summarizing G-banding of ESC lines derived from control and ST blastocysts.

DETAILED DESCRIPTION

Provided herein is a method of generating a viable human oocyte, the method comprising the steps of:

a) enucleating a first oocyte at the MII stage, thereby creating a cytoplast;
b) isolating a polar body from a second oocyte by aspiration; and
c) placing the polar body into the perivitelline space thereby fusing the polar body with the cytoplast and generating the viable human oocyte.

In other embodiments, the methods herein involving polar body transplantation further comprise a step of fertilizing the viable human oocyte via in vitro fertilization, thereby creating an embryo. In further embodiments, the method further comprises implanting the embryo in a receptive endometrial uterine lining.

In other embodiments of the methods, enucleating the first oocyte is performed in a medium comprising at least 10% human tubal fluid, HEPES buffer, and cytochalasin B. In other embodiments the enucleation step is completed using a Polarized Microscope Imaging System.

In still further embodiments, the method step for isolating the polar body is performed in a medium comprising at least 10% human tubal fluid, HEPES buffer, cytochalasin B, and fusion with donor cytoplast induced with HVJ-E extract.

I other embodiments, the zona pellucida is opened via methods selected from zona cutting, laser drilling (such as with a compact nitrogen laser), and acid drilling (such as with acidic Tyrode's medium).

Also provided is a method of producing a human oocyte in vitro, the method comprising:

a) determining a mitochondrial DNA sequence of the conserved sequence box II of a donor oocyte;
b) enucleating the donor oocyte while the donor oocyte is arrested at metaphase II, thereby isolating donor nuclear genetic material;

c) introducing the donor nuclear genetic material into an enucleated recipient oocyte, provided that the mitochondrial DNA of the donor oocyte has the same conserved sequence box II genotype as the recipient oocyte.

In some embodiments, the method immediately above is accomplished where the donor oocyte and the recipient oocyte both have the G5A8 genotype or both have the G6A8 genotype. In still other embodiments of the method the mitochondrial DNA from the donor oocyte comprises a mutation that results in a mitochondrial disease, including but not limited to Leigh Syndrome or MELAS.

Also provided is a method of producing a human oocyte in vitro, the produced human oocyte comprising minimal maternal mitochondrial DNA, and the method comprising the steps of:

a) determining the sequence of the major non-coding region of the mitochondrial DNA of a donor oocyte, where the major non-coding region sequence includes a D loop region;
b) enucleating the donor oocyte while the donor oocyte is arrested at metaphase II, thereby isolating donor nuclear genetic material; and
c) introducing the donor nuclear genetic material into an enucleated recipient oocyte, provided that the mitochondrial DNA of the donor oocyte has the same major non-coding region sequence as the recipient oocyte.

In further embodiments of the method immediately above the donor oocyte and the recipient oocyte both have the H56, H1b, U5a, F1a, X2c, D4a, H49, or B2k mtDNA haplotype. In other embodiments, the mitochondrial DNA from the donor oocyte comprises a mutation that results in a mitochondrial disease, such as Leigh Syndrome or MELAS.

Other mitochondrial diseases for which use of the present methods may be considered include, but are not limited to, possible occurrence of mitochondrial myopathy; diabetes

mellitus and deafness; progressive infantile poliodystrophy (Alpers disease); Leber's hereditary optic neuropathy; Barth Syndrome/Lethal Infantile Cardiomyopathy (LIC); neuropathy, ataxia, retinitis pigmentosa, and ptosis (NARP); myoneurogenic gastrointestinal encephalolpathy (MNGIE); carnitine-acyl-carnitine deficiency; carnitine deficiency; creatine deficiency syndromes; Co-enzyme Q10 deficiency; Complex I deficiency; Complex II deficiency; Complex III deficiency; Complex IV deficiency/COX deficiency; Complex V deficiency; myoclonic epilepsy with ragged red fibers (MERRF); mitochondrial myopathy, encephalomyopathy, lactic acidosis, stroke-like-symptoms (MELAS); mtDNA depletion; Chronic Progressive External Ophthalmoplegia Syndrome (CPEO); CPT I Deficiency; CPT II Deficiency; Kearns-Sayre Syndrome (KSS); lactic acidosis; LBSL-Leukodystrophy; Long-Chain Acyl-CoA Dehydrogenase Deficiency (LCAD); :LCHAD; Luft Disease; Multiple Acyl-CoA Dehydrogenase Deficiency; Short-Chain Acyl-CoA Dehydrogenase Deficiency; Medium-Chain Acyl-CoA Dehydrogenase Deficiency; Very Long-Chain Acyl-CoA Dehydrogenase Deficiency; Mitochondrial Encephalomyopathy Lactic Acidosis and Stroke-like Episodes (MELAS); Mitochondrial Recessive Ataxia Syndrome; Mitochondrial Cytapathy; Mitochondrial DNA Depletion; Mitochondrial encephalopathy; Myoneurogastrointestinal Disorder and Encephalopathy; Pearson Syndrome; Pyruvate Carboxylase Deficiency; Pyruvate Dehydrogenase Deficiency; and POLG2 Mutations.

Definitions

The term "polar body" refers to haploid cells, significantly smaller than an oocyte that is formed in conjunction with an oocyte during oogenesis. In particular, polar bodies include the half of the diploid chromosome set not included in the oocyte after meiotic division. Polar bodies comprise polynucleotides (*e.g.*, DNA) that encode information about the individual. Nuclear genetic material includes, but is not limited to, chromosomes and chromatin. The term includes nuclear genetic material produced by meiotic cell division such as the division or a diploid cell to a haploid oocyte. Thus, a cell includes nuclear genetic material derived from a donor polar body if the polar body has been transferred into an enucleated cytoplast via somatic cell nuclear transfer.

The term "oocyte" refers to a female gamete or germ cell involved in reproduction, also called an egg. A mature oocyte is a haploid cell with a single set of maternal chromosomes (23, X in a human primate) and is halted at metaphase II. A "hybrid" oocyte has the cytoplasm from a first primate oocyte (termed a "recipient") but does not have the nuclear genetic material of the recipient; it has the nuclear genetic material from another oocyte or a polar body and is termed a "donor" oocyte.

Meiosis is a process of reductional division in which the number of chromosomes per cell is halved. In animals, meiosis always results in the formation of gametes. During meiosis, the genome of a diploid germ cell, which is composed of long segments of DNA packaged into chromosomes, undergoes DNA replication followed by two rounds of division, resulting in four haploid cells. Each of these cells contain one complete set of chromosomes, or half of the genetic content of the original cell. Meiosis I separates homologous chromosomes, producing two haploid cells (23 chromosomes, N in humans), so meiosis I is referred to as a reductional division. A regular diploid human cell contains 46 chromosomes and is considered 2N because it contains 23 pairs of homologous chromosomes. However, after meiosis I, although the cell contains 46 chromosomes it is only considered N because later in anaphase I the sister chromatids will remain together as the spindle pulls the pair toward the pole of the new cell. In meiosis II, an equational division similar to mitosis occurs whereby the sister chromatids are finally split, creating a total of 4 haploid cells (23 chromosomes, N) per daughter cell from the first division.

A "meiotic spindle" is a structure that separates the chromosomes into daughter cells during meiotic cell division. It is part of the cytoskeleton in eukaryotic cells. The spindle apparatus includes the spindle microtubules, associated proteins, and any centrosomes or asters present at the spindle poles. The spindle apparatus is vaguely ellipsoid in shape and tapers at the ends but spreads out in the middle. In the wide middle portion, known as the spindle midzone, antiparallel microtubules are bundled by kinesins. At the pointed ends, known as spindle poles, microtubules are nucleated by the centrosomes in most animal cells.

The term "mitochondrial DNA" or "mtDNA" refers to the DNA of the mitochondrion, a structure situated in the cytoplasm of the cell rather than in the nucleus (where all the other chromosomes are located). In vivo, all mtDNA is inherited from the mother. There are 2 to 10 copies of the mtDNA genome in each mitochondrion. Mitochondrial DNA is a double-stranded, circular molecule. It is very small relative to the chromosomes in the nucleus and includes only a limited number of genes, such as those encoding a number of the subunits in the mitochondrial respiratory-chain complex and the genes for some ribosomal RNAs and transfer RNAs. A cell includes mtDNA derived from the continued replication cytoplasmically based mitochondria, which in the case of polar body transfer are based in the recipient cytoplast.

The term "DNA methylation" refers to the postsynthetic addition of methyl groups to specific sites on DNA molecules; the reaction is catalyzed by enzymes called DNA methyltransferases that are specific for nucleotide and position of methylation. In eukaryotes, methylation is involved in gene expression, and plays a role in a variety of epigenetic mechanisms, including development, X chromosome inactivation, genomic imprinting, mutability of DNA, and uncontrolled cell growth in cancer.

The term "X chromosome inactivation" refers to the inactivation of one of each pair of X chromosomes to form the Barr body in female mammalian somatic cells. Thus tissues whose original zygote carried heterozygous X borne genes should have individual cells expressing one or other but not both of the X encoded gene products. The inactivation is thought to occur early in development and leads to mosaicism of expression of such genes in the body.

The phrase "dosage compensation" refers to a mechanism that senses gene dosage and regulates expression accordingly. In mammals there is monoallelic expression of X-linked genes that differ in dose between females (XX) and males (XY). "XIST" refers to a gene encoding a large non-coding RNA which has been shown to be necessary for developmentally regulated X chromosome silencing in females. The XIST RNA is about 18 kb and is not translated, it is spliced, and polyadenylated. It is also organized into blocks of repetitive sequence. In vivo, XIST RNA is found to be stably associated with the silenced X chromosome. The expression of XIST RNA is always cis-limited, and is associated with the silenced X chromosome in females.

The term "effective amount" or "therapeutically effective amount" refers to the amount of agent or a cell that is sufficient to prevent, treat, reduce and/ or ameliorate the symptoms and/or underlying causes of any disorder or disease, or the amount of an agent sufficient to produce a desired effect on a cell. In one embodiment, a "therapeutically effective amount" is an amount of a cell or an agent sufficient to reduce or eliminate a symptom of a disease. In another embodiment, a therapeutically effective amount is an amount sufficient to overcome the disease itself.

As used herein, the term "embryo" refers generally to a cellular mass obtained by one or more divisions of a zygote or an activated oocyte with an artificially reprogrammed nucleus. A "morula" is the preimplantation embryo 3-4 days after fertilization, when it is a solid mass, generally composed of 12-32 cells (blastomeres). A "blastocyst" refers to a preimplantation embryo in placental mammals (about 3 days after fertilization in the mouse, about 5 days after fertilization in humans) of about 30-150 cells. The blastocyst stage follows the morula stage, and can be distinguished by its unique morphology. The blastocyst is generally a sphere made up of a layer of cells (the trophectoderm), a fluid-filled cavity (the blastocoel or blastocyst cavity), and a cluster of cells on the interior (the ICM).

"Nuclear transfer" refers to the insertion of a donor polar body nucleus into an enucleated recipient host cell.

Unless otherwise explained, all technical and scientific terms used herein have the same meaning as commonly understood by one of ordinary skill in the art to which this disclosure belongs. The singular terms “a,” “an,” and “the” include plural referents unless context clearly indicates otherwise. Similarly, the word “or” is intended to include “and” unless the context clearly indicates otherwise. It is further to be understood that all base sizes or amino acid sizes, and all molecular weight or molecular mass values, given for nucleic acids or polypeptides are approximate, and are provided for description. Amounts that are “about” a given numeric range or value include the exact numeric range or value. Although methods and materials similar or equivalent to those described herein can be used in the practice or testing of this disclosure, suitable methods and materials are described below. The term “comprises” means

"includes." All publications, patent applications, patents, and other references mentioned herein are incorporated by reference in their entirety. In case of conflict, the present specification, including explanations of terms, will control. In addition, the materials, methods, and examples are illustrative only and not intended to be limiting.

The development of normal, competent, haploid oocytes depends on two consecutive meiotic cell divisions in the absence of an intermediate DNA replication S-phase (Petronczki et al., 2003). In mammals, primordial germ cells form primary oocytes that undergo chromosome recombination during fetal development and then arrest at prophase of meiosis I. Meiosis is resumed, in turn, in selected primary oocytes after puberty, during periodic menstrual cycles, leading to completion of the first meiotic division, abstriction of PB1 and formation of a secondary oocyte that arrests again at metaphase of meiosis II. MII resumes post-ovulation, during fertilization, resulting in segregation of second polar body (PB2) and the formation of a haploid oocyte genome (Clift D and Schuh M, *Mol Cell Biol* **14**, 549-562 (2013); incorporated by reference herein). Haploid DNA contributions from sperm and egg intermingle during preparation for the first mitotic division and completion of fertilization.

Interphase nuclei of skin fibroblasts transplanted into enucleated human MII oocytes (cytoplasts) undergo rapid remodeling and cell cycle reprogramming resulting in the formation of oocyte-like MII-arrested spindles (Ma H *et al*, *Nature* **511**, 177-183 (2014); Tachibana M *et al*, *Cell* **153**, 1228-1238 (2013); both of which are incorporated by reference herein). Residual meiotic activity in cytoplasts capable of forming *de novo* MII spindles is critical for reprogramming and subsequent embryonic development following somatic cell nuclear transfer (SCNT). Since the main purpose of human SCNT is to produce autologous ESCs, MII-arrested SCNT oocytes are not fertilized with sperm but activated artificially to exit meiotic arrest, while segregation of chromosomes during the second meiotic division is suppressed to preserve the diploid somatic cell genome. The reprogramming potential of meiotic oocyte cytoplasm, as demonstrated by SCNT, suggested the possibility of producing haploid oocytes with donor genomes in the context of a treatment for infertility. Previous mouse studies demonstrated that both PB1 and PB2 genomes can be reconstituted by transfer into compatible MII or zygotic

cytoplasm and contribute to development of viable offspring (Wakayama T *et al*, *J Reprod Fertil* **110**, 263-266 (1997); Wakayama T and Yanagimachi R, *Biol of Reproduction* **59**, 100-104 (1998); incorporated by reference herein). However, these murine studies have not been translated to other species including primates and humans. Disclosed herein is the generation of haploid human oocytes following transfer of PB1 genomes into enucleated MII oocytes and induction of *de novo* meiosis II after fertilization with sperm (**Figure 1A**). Preimplantation development of PBNT oocytes to blastocysts and ESCs was also studied and their genetic and epigenetic properties determined.

Previous mouse studies demonstrated that both polar body genomes retain the potential to participate in normal development or form ESCs if reintroduced into corresponding oocyte or zygotic cytoplasm (Wakayama S *et al*, *Stem Cells* **25**, 986-993 (2007) and Wang T *et al*, *Cell* **157**, 1591-1604 (2014); both of which are incorporated by reference herein). Disclosed herein is the translation of these mouse discoveries and the demonstration that PBNT can rescue the genetic material of developmentally discarded human PB1 genomes. Residual meiotic activity in enucleated MII oocytes is sufficient to induce formation of *de novo* functional, MII-like spindles that result in haploid oocyte upon fertilization. Using noninvasive birefringence imaging, it was found that most PBNT oocytes (67%) formed visible spindles within 60 min of fusion. However, more detailed spindle morphology analysis in stained oocytes revealed that some meiotic spindles were at prophase or anaphase, suggesting compromised nuclear content in PB1. Furthermore, approximately half of normally fertilized PBNT zygotes arrest before reaching the blastocyst stage, suggesting that efforts to optimize protocols in the timing of oocyte harvest for isolating viable PBs are appropriate.

Aneuploidy in IVF embryos is relatively common (Alfarawati S *et al*, *Fertil Steril* **95**, 520-524 (2011) and Angell RR *et al*, *Nature* **303**, 336-338 (1983); incorporated by reference herein) and, as shown here, also occurs in PBNT blastocysts. Aneuploidy rates in human embryos increase with maternal age as a result of meiosis I or II errors (Hassold T and Hunt P, *Nat Rev Genet* **2**, 280-291 (2001); Nagaoka SI *et al*, *Nat Rev Genet* **13**, 493-504 (2012); Petronczki M *et al*, *Cell* **112**, 423-440 (2003); incorporated by reference herein). In addition, mitotic errors

during-post zygotic cleavage divisions may occur, producing mosaic blastomeres containing multiple distinct karyotypes within a preimplantation embryo (McCoy RC *et al*, *PLoS Genetics* **11**, e1005601 (2015); incorporated by reference herein). While PBNT is unlikely to correct meiosis I errors, functional cytoplasm from young donors may reduce incidences of aneuploidy resulting from meiosis II or mitotic errors. Aneuploidy rates in normally fertilized PBNT blastocysts in the current study were similar to controls based on STR and Array-CGH analyses. It is likely that that further optimizations of PBNT protocols will reduce aneuploidy rates. Nevertheless, implementing preimplantation genetic screening (PGS) is critical prior to clinical applications of PBNT oocytes.

Due to the current trend toward delayed childbearing in the Western world, age-related infertility with concomitant decreases in ovarian reserve is common (Bellieni CV, *World J Clin Pediatr* **1**, 34-36 (2012); incorporated by reference herein). It is disclosed herein that generating additional oocytes by rescuing PB1 would increase the yield of patient-related blastocysts available for transfer from a single stimulation cycle. This implies that utilization of PBNT may significantly improve ART outcomes and pregnancy rates, particularly for women of advanced age with decreased ovarian reserve. However, this therapy is based on availability of patient PB1, and therefore, is not applicable for women who cannot produce mature oocytes (Bilgin EM and Kovanci E, *Curr Opin Obst Gynecol* **27**, 167-174 (2015); Grynberg M *et al*, *Fertil Steril* **105**, 13-19 (2016); both of which are incorporated by reference herein). Moreover, PBNT technology will be limited to countries, such as the United States, where IVF programs are allowed to coordinate oocyte donation cycles with compensation of donors. Polar body biopsy is an established technique in IVF and its removal from patient oocytes does not affect fertilization and subsequent embryo development (Cimadomo D *et al*, *Biomed Res Int* **2016**, 7193075 (2016). Since PBNT relies on donor oocytes, this strategy allows complementation of PB genomes from older women with young donor cytoplasts.

Expanded use of PBNT, in addition to spindle transfer (ST), could provide an additional technique to support mitochondrial replacement therapy (MRT); a promising approach to avoid maternal transmission of mtDNA-based disease (Tachibana M *et al*, *Nature* **493**, 627-631 (2013)

and Tachibana M *et al*, *Nature* **461**, 367-372 (2009); both of which are incorporated by reference herein). In mice, it has been demonstrated that a minimal mtDNA carryover can be achieved in offspring generated by polar body transfer (Wang T *et al*, *Cell* **157**, 1591-1604 (2014) and Yamada M *et al*, *Cell Stem Cell* **18**, 749-754 (2016); both of which are incorporated by reference herein). Disclosed herein is data suggesting that in conjunction with ST, PBNT could potentially increase the number of reconstructed MRT oocytes for families with mtDNA-based defects. Similar to other MRT technologies, PBNT will have to meet safety and efficacy requirements of regulatory agencies before approval for routine clinical applications (Wolf DP *et al*, *Trends Mol Med* **21**, 68-76 (2015); incorporated by reference herein). In addition, PBNT provides a tool to study basic mechanisms of developmental biology related to female meiosis and expands the understanding of the genetic stability in oocytes.

EXAMPLES

The following examples are for illustration only. In light of this disclosure, those of skill in the art will recognize that variations of these examples and other examples of the disclosed invention be possible without undue experimentation.

Example 1 - De novo formation of MII spindles from the PB1 genomes

It was first determined whether the residual meiotic activity in enucleated human MII oocytes is sufficient to induce formation of morphologically normal MII-like spindles from the PB1 genome, carrying a genetic complement of MII chromosomes (Hou Y *et al*, *Cell* **155**, 1492-1506 (2013); incorporated by reference herein). To this end, fresh MII oocytes donated by and retrieved from 11 healthy volunteers (25-31 years) were used following controlled ovarian stimulation (COS) protocols and transvaginal follicular aspirations.

Using immunochemistry with antibodies against α and β tubulins and 4',6-diamidino-2-phenylindole (DAPI) for DNA staining, it was determined that intact PB1s in mature, human MII oocytes do not contain detectable metaphase spindles, possibly due to a rapid decline in meiotic factors after abstriction (**Figure 1B**). Reconstructed PBNT oocytes were produced by fusing intact, round PB1 with MII cytoplasts (**Figures 1A and 1C**). Noninvasive imaging indicated

that most PBNT oocytes (67%) formed visible spindles within 60 min of fusion (**Figure 1D**). Labeling with antibodies for α and β tubulins and DAPI demonstrated that all PBNT oocytes (n=5) contained spindle-chromosomal complexes. However, only 2 experimental oocytes formed metaphase spindles similar to intact MII oocytes. The remaining PBNT spindles were at prophase (n=2) or anaphase (n=1) (**Figure 1B**) likely reflecting compromised nuclear content.

Example 2 - Resumption and completion of meiosis II in PBNT oocytes following fertilization with sperm

When the functionality of meiotic spindles in reconstructed PBNT oocytes was examined post-fertilization, by intracytoplasmic sperm injection (ICSI), completion of meiosis II was evidenced by the abstriction of PB2 and formation of pronuclei. Most PBNT oocytes survived ICSI (97%; 31/32) and formed visible pronuclei (81%; 25/31) at rates similar to non-manipulated intact controls (**Table 1**). The majority of fertilized PBNT zygotes (76%; 19/25) contained 2 pronuclei (PN) and a second polar body (PB2) indicative of normal meiosis II completion (Figure 1E). The remaining zygotes carried irregular numbers of pronuclei (1 or 3) or failed to extrude PB2 (**Figure 1E; Table 1**). These outcomes were slightly lower than the control (**Table 1**) indicative that the majority of PBNT oocytes form functional spindles capable of recapitulating meiosis II after fertilization.

Table 1

Completion of Meiosis II in PBNT and Intact, Control MII Oocytes after Fertilization

Group	No. of oocytes	Survival after ICSI (%)	Fertilization rate (%)	Normal meiosis II completion (%)	Abnormal meiosis II completion		
					3 PN (%)	1PN (%)	2PN/0PB (%)
PBNT	32	31/32, (97±1)	25/31, (81±8)	19/25, (76±10)	2/25, (8±10)	2/25, (8±5)	2/25, (8±7)
Control	21	20/21, (95±6)	17/20, (85±8)	16/17, (94±4)	0/17, (0)	1/17, (6±4)	0/17, (0)

Example 3 - Preimplantation development and ploidy of PBNT blastocysts

To examine developmental competency, normally fertilized PBNT zygotes and controls were cultured to the blastocyst stage. Similar to controls, 95% (18/19) of PBNT zygotes cleaved, 74% (14/19) reached 8-cell and 68% (13/19) formed compact morula stage embryos (**Table 2**). In the control group, 75% (12/16) of the zygotes reached blastocysts while only 42% (8/19) of PBNT zygotes did (Student's *t*-test, $p < 0.05$, **Figure 1F, 1G and Table 2**). Since embryonic

aneuploidy resulting from numerical chromosomal abnormalities leading to implantation failure or spontaneous pregnancy loss is common irrespective of blastocyst morphology, selected PBNT (n=2) and control (n=3) blastocysts were subjected to short tandem repeat (STR) analysis. Examination of microsatellite markers mapping to 22 human autosomal loci and one X-linked locus revealed that two sampled PBNT blastocysts contained normal diploid chromosomes contributed from both oocyte and sperm. These results minimized the possibility of errors in oocyte meiotic chromosomal segregation. Three additional PBNT blastocysts were subjected to trophectoderm biopsy and performed array comparative genomic hybridization (Array-CGH) analysis and determined that two were normal but one blastocyst was aneuploid (loss of 17). This outcome was comparable to controls with one aneuploid blastocyst out of three tested (loss of 21).

Table 2

Preimplantation Development of PBNT and Control Zygotes

Group	No. of oocytes with normal meiosis II completion	2 cell (%)	8 cell (%)	Compact morula (%)	Blastocyst (%)
PBNT	19	18/19, (95±2)	14/19, (74±17)	13/19, (68±18)	8/19, (42±9)[a]
Control	16	16/16, (100)	15/16, (96±4)	14/16, (88±5)	12/16, (75±10)[b]

[a, b] Different superscripts within a column indicate significant differences ($P < 0.05$).

Example 4 - Genetic integrity in ESCs derived from PBNT embryos

In an effort to further define the potential clinical utility of reconstructed, haploid PBNT oocytes, one ESC line was derived from five PBNT blastocysts. The line was designated PBNT1 (**Figure 1F**). An additional four ESC lines were developed from nine control blastocysts. This included hESO-14, which was a genetically related sibling of PBNT1, derived from the same egg and sperm donors. Lower ESC derivation efficiency (20%, 1/5) from PBNT embryos compared to controls (44%, 4/9) may indicate poor quality of PBNT blastocysts but total numbers were low for definitive conclusions. One ESC line (PBNT2) was derived from two blastocysts grown from abnormal (3PN) PBNT zygotes. Cytogenetic G-banding revealed that PBNT1 and three of the

four control ESCs exhibited normal diploid karyotypes with no evidence of detectable numerical or structural chromosomal abnormalities (**Figure 2A**). The remaining control hESO-15 was aneuploid with chromosome 21 monosomy (**Figure 2A)**. In addition, STR analysis of PBNT1 and hESO-14 confirmed their normal ploidy and sibling relationship (**Table 3**). As expected, PBNT2 displayed a 66-69, XXX triploid karyotype (**Figure 2A**). DNA fingerprinting by STR corroborated the presence of three alleles for chromosomes 2, 6, 13, 18, and 22 and four alleles on chromosome 12 in this cell line (**Table 3**). On the basis of allelic inheritance analysis, the triploid karyotype was caused by failed meiosis II completion with retention of PB2 genetic material. This was consistent with observation of 3 pronuclei and failure to segregate a second polar body after fertilization in these zygotes. In addition, the sperm also contributed a second allele to chromosome 12 tetraploidy. Both PBNT1 and control hESO-14 lines maintained typical ESC morphology and formed teratoma tumors containing cells and tissues from all three germ layers (**Figures 5A and 6B).**

Table 3

Parentage Analysis of PBNT1, PBNT2, and hESO-14 Determined by Short Tandem Repeat (STR) Assay

STR loci	PBNT1	hESO-14	Oocyte donor1	Sperm donor1	PBNT2	Oocyte donor2	Sperm donor2
Sex AME	F XX	F XX	F XX	M XY	F XXX	F XX	M XY
D1S548	152/176	152/176	152/168	168/176	168/172	152/168	152/172
D2S1333	297/301	289/317	297/317	289/301	285/301/305	285/301	305/305
D3S1768	192/200	192/200	200/200	192/192	188/196	188/196	196/200
D4S2365	296/300	296/296	296/300	296/296	296/300	296/300	296/296
D4S413	123/161	123/125	125/161	123/123	123/125	123/123	123/125
D5S1457	123/123	101/105	101/123	105/123	119/123	123/123	119/123
D6S276	227/249	227/249	249/251	227/235	227/235/237	227/235	237/251
D6S501	164/172	164/172	172/172	164/168	164/168/172	168/172	164/172
D11S2002	254/254	254/254	254/254	254/254	254/254	254/254	254/254
D11S925	299/300	297/300	282/300	297/299	282/305	305/305	282/282
D12S364	264/286	264/286	276/286	264/274	270/272/274	270/272	270/274
D12S67	248/260	248/260	252/260	248/264	252/256/260/264	252/260	256/264
D13S765	188/200	188/196	188/192	196/200	188/192/200	188/200	188/192
D16S403	143/145	137/145	145/145	137/143	135/145	145/145	135/149
D17S1300	261/265	261/265	265/265	249/261	265/269	257/269	257/265
D18S537	204/204	204/204	200/204	204/204	196/200/208	196/208	200/204
D18S72	301/305	301/307	301/305	305/307	301/305	301/305	301/305
D22S685	184/188	184/188	188/188	184/188	180/192/196	180/192	192/196
DXS2506	278/282	278/282	282/282	278*	183/183	183/199	183*
MFGT22	104/108	104/104	104/108	104/108	108/108	108/112	108/108

* Only male samples show one mark of DXS2506 on X chromosome.

To evaluate if PBNT introduced subchromosomal changes undetectable by G-banding, genome-wide, high-resolution genome physical maps of PBNT1 and hESO-14 lines, as well as

the egg and sperm donor DNA were generated. The BioNano Genomics Irys platform (Mak AC *et al*, *Cell Stem Cell* **5**, 11-14 (2016); incorporated by reference herein) enables detection of structural variations (SVs) including insertions, deletions and inversions at 1-kb resolution. When compared to the egg donor genome, 372 SVs were identified in PBNT1 and 380 SVs in hESO-14, of which 157 were shared between these sibling cell lines (**Figure 2B**). Compared to the sperm donor genome, 268 SVs were detected in PBNT1 and 265 SVs in hESO-14 with 124 common SVs (**Figure 2C**). In addition, comparable numbers of unique SVs were identified in PBNT1 (281) and hESO-14 (297) (**Figure 2D**). No genes were found within or close to SVs that were differentially expressed between PBNT1 and hESO-14.

Example 5 - Epigenetic and transcriptional signatures of PBNT ESCs

DNA methylation involving the covalent transfer of a methyl group to the fifth carbon atom of the cytosine ring is an important epigenetic mechanism defining cell identity (Smith ZD and Meissner A, *Nat Rev Genet* **14**, 204-220 (2013); incorporated by reference herein). This process undergoes dynamic changes during and after fertilization reflecting developmental reprogramming (Canovas S and Ross PJ, *Theriogenology* **86**, 69-79 (2016); incorporated by reference herein). Also, the establishment of stable ESCs is associated with major changes in methylation profiles as the genome reconfigures to the pluripotent state (Lister R *et al*, *Nature* **462**, 315-322 (2009); Lister R *et al*, *Nature* **471**, 68-73 (2011); both of which are incorporated by reference herein). To evaluate the normalcy of these changes, genome-wide DNA methylation analyses of PBNT1 and hESO-14 cell lines were conducted using high-coverage, base-resolution MethylC-seq (Lister 2009 *supra*). Both lines showed similar levels of CG methylation, a difference of only 0.7% between PBNT1 (86.1%) and hESO-14 (85.4%), and non-CG methylation, a difference of only 0.4% between PBNT1 (1.3%) and hESO-14 (0.9%) (**Figure 3A and 3B**). Pairwise comparison of these two samples identified only 116 CG differentially methylated regions (DMRs) and 4 non-CG mega DMRs spanning about 500kb (He Y and Ecker JR, Ann Rev Genom Hum Genet 16, 55-77 (2015); incorporated by reference herein) (**Figure 3C; Table S5,** FDR < 0.01). Visual inspection implied the conformation of these DMRs (**Figure 3D and 3E**), but there was no enrichment in gene ontology (GO) terms, genetic features (**Figure 3C**), or

correlation to the transcriptional profile. These outcomes suggest that the global methylation profile of experimental PBNT1 appeared very similar to control hESO-14.

Finally, global gene expression patterns were examined in the PBNT1 and hESO-14 lines. Deep sequencing (50M reads) by RNA-seq was performed in triplicates for each of the two lines. Differential expression analysis was performed using the edgeR package (Robinson MD and Smyth GK, *Biostatistics* **9**, 321-332 (2008); incorporated by reference herein) and showed that only 1.25% of the examined genes (186 out of 14,876) were differentially expressed between PBNT1 and hESO-14 (**Figures 4A and 4B,** FDR < 0.05). Using Gene Ontology (GO) analysis, various GO terms were allocated. However, no statistically enriched functional categories for the differentially expressed genes were identified. These data indicated that the global gene expression patterns of PBNT1 cells closely resembled those of control hESO-14 cells.

Thus, within the limits of these analyses, the PB1 genome interacts with oocyte cytoplasm establishing epigenetic and transcriptome characteristics that emulate the pluripotent state.

Example 6 – Gamete Donation

Oocyte donors 25-31 years of age were recruited through the OHSU Women's Health Research Unit. Two healthy sperm donors were also recruited. Eligible participants attended an information session describing study goals and related procedures. Written informed consent was obtained from all gamete donors stating that oocytes will be fertilized to create embryos for research purposes and will not be used for reproductive purposes but rather will be studied in vitro including generation of embryonic stem cells.

Example 7 – Methods

To produce recipient MII cytoplasts, oocytes were placed into a 50 µl manipulation droplet of human tubal fluid with HEPES 10% medium containing 5 µg/ml cytochalasin B (HTF w/HEPES 10% CB) in a glass bottom dish. The droplet was covered with tissue culture oil and oocytes were maintained at 37 °C for 10 min before enucleation. The dish was mounted on the stage of an inverted microscope (Olympus IX71) equipped with a stage warmer

(http://www.tokaihit.com), Narishige micromanipulators, Oosight Imaging System (http://wwwcri-inc.com), and laser objective (http://www.hamiltonthome.com) (websites and contents incorporated by reference herein). An oocyte was positioned using a holding pipette so that the spindle was situated at a position of about 2-4 o'clock. The zona pellucida next to the spindle was laser drilled and then an enucleation pipette was introduced through the slit. The spindle was extracted by aspiration into the pipette with a minimal amount of cytoplasm and surrounding plasma membrane and discarded.

For polar body isolation, an oocyte was positioned with the first polar body (PB1) at 2 o'clock, and the zona pellucida was drilled before a transfer pipette was introduced and the PB1 aspirated. The PB1 was then transferred briefly into a drop containing HVJ-E extract (Ishihara Sangyo Kaisha) diluted 1:3 with HTF w/HEPES 10% CB, transferred and rinsed in HTF w/HEPES 10% CB, and placed in the perivitelline space of the recipient cytoplast. The couplets were rinsed in HTF w/HEPES 10%, transferred to Global 10% medium, and incubated at 37 °C in 6% CO_2 for 60 min to allow fusion. Fusion was confirmed 30-60 min after nuclear transfer and PBNT oocytes were fertilized after an additional 50 min culture using intracytoplasmic sperm injection (ICSI) using fresh donor sperm. Fertilized oocytes were then cultured in Global10% medium at 37 °C in 6% CO_2, 5% O_2 and 89% N_2. Fertilization was determined 16 hours after ICSI by noting pronuclear formation and polar body extrusion. Non-manipulated intact Mil oocytes served as controls that were fertilized and cultured similar to the PBNT group.

The following examples also help demonstrate examples within the present scope in regard to oocytes prepared to overcome problems with poor mitochondrial genomics.

Example 8 – Inclusion and Exclusion Criteria

Since mitochondrial disease can be attributed to genome mutations in mtDNA and/or nuclear DNA (Wallace DC, *J Clin Invest* 123, 1405-1412 (2013); incorporated by reference herein), an important clinical challenge is to confirm pathogenic mtDNA mutations in families eligible for MRT. Five families - four diagnosed with Leigh syndrome (LS) and one with MELAS - were recruited and genetic testing performed to confirm maternally inherited mtDNA mutations. DNA was collected from blood, skin fibroblasts (SF) and/or urine from children and

mothers, and whole mtDNA sequencing was performed. The first LS family had an affected 2-year-old child with a homoplasmic T8993G substitution in both blood and SF samples while her 22-year-old mother had the same mutation with 70% heteroplasmy in blood and 100% in SF (Figure 6A, left).

In the second related LS family, an affected 2.5-year old child carried the same T8993G mutation at 95% heteroplasmy in blood and 100% in SF while in a second 1-year old asymptomatic sibling, the mutation load was 50% in blood and 62% in SF. Their 23-year-old mother, who was the elder sister of the subject from the first family, carried this mutation at 13% in blood and 16% in SF (Figure 6A, right).

In the third LS family, the affected 12-year-old boy harbored a G13513A substitution at 56%, 86% and 97% heteroplasmy in blood, SF and urine, respectively. His asymptomatic 19-year-old brother carried same mutation at 10%, 14% and 23% heteroplasmy levels in blood, SF and urine, respectively. Their 36-year-old mother also harbored the mutation at 3%, 98% and 39% levels in blood, SF and urine, respectively (Figure 6B).

A fourth family also presented with a 1-year-old child diagnosed with LS. However, genetic screening did not reveal any pathogenic mtDNA mutations in the child or mother.

The fifth family was from a large, well-studied MELAS pedigree carrying a pathogenic A3243G mutation (Figure 10B) (McClelland K, 2014, https://scholarworks.csustan.edu/bitstream/handle/011235813/793/McClellandK.summer2014%20.pdf?sequence=1; website last accessed 28 Nov 2016 and incorporated by reference herein). The 32-year-old mother carried the mutation at 14%, 47% and 35% in blood, SF and urine, respectively. All her 3 children inherited this mutation (Figure 6C).

These results indicated that maternally transmitted, pathogenic mtDNA mutations were implicated in four of the five families studied. The clinical LS phenotype in the fourth family was not associated with any pathogenic mtDNA mutation and thus was excluded from further analyses. This highlights the importance of genetic testing for maternally inherited mtDNA diseases prior to MRT. Moreover, since heteroplasmy levels may vary among different tissues,

it is critical to sample and test blood, skin and urine, in both mothers and children (Monnot S *et al*, *Hum Mutat* 32, 116-125 (2011); incorporated by reference herein).

Healthy volunteer oocyte donors were also screened and it was confirmed that they did not carry any inherited pathogenic mtDNA mutations. Their mtDNA sequences and corresponding haplotype were subsequently used for matched MRT combinations.

Example 9 – COS (controlled ovarian stimulation), oocyte recovery and mutations in oocytes

Women with mtDNA disease display live birth rates comparable to the general population, therefore, it is accepted that they have normal fertility. However, ovarian response to gonadotropin stimulation and oocyte recovery in women carrying pathogenic mtDNA mutations (carriers) was assessed.

Age was similar between carrier and healthy donors. AMH levels, a measure of ovarian reserve, were lower in carriers than in healthy donors (1.1 vs. 4.8 ng/ml). Antral follicle count (AFC) was also lower in carriers compared to the healthy donors (10.3 vs. 22.3). In addition, the duration of COS was about one day longer in the carriers and their peak blood estradiol (E2) level prior to hCG administration also trended lower. Finally, the total number and the number of mature MII oocytes retrieved were also significantly lower in carriers (5.8 vs. 16.6 and 3.8 vs. 13.2, respectively) (Figures 11A, 11B, 11C, 11D, 11E, 11F, and 11G). Of note, one carrier (cED2) exhibited premature luteinization, as evidenced by increased progesterone levels prior to the LH surge (Figure 11H). Therefore, mutation analyses were performed only on retrieved atretic oocytes.

Although the numbers in the cohort were low (Smeets HJ *et al*, *Ann NY Acad Sci* 1350, 29-36 (2015); incorporated by reference herein), the results suggest that mtDNA mutation could lead to reduced ovarian response. Older age and higher BMI in carriers could also have affected the outcome (Kelsey TW *et al*, *PLoS One* 6, e22024 (2011) and Kelsey TW *et al*, *Mol Hum Reprod* 18, 79-87 (2012); both of which are incorporated by reference herein). Another potential contributing factor is the long-term hormonal contraception these women were on prior to ovarian stimulation.

MtDNA mutations were then identified in individual oocytes from the carriers. After MII spindle (nuclear genome) removal, the cytoplasts (mtDNA) were used for sequencing. In the first carrier, two recovered oocytes carried the T8993G mutation at 86% and 96% levels. In the second sibling carrier, heteroplasmy levels in 5 atretic oocytes ranged from 72% to 100%. In 4 oocytes from the third LS carrier, the G13513A mutation levels in 3 eggs were very low (0.6 - 3%) while the fourth was at 40%. Finally, in nine oocytes from the A3243G MELAS carrier, the mutation was not detected in one egg while the remaining carried 9-52% (Figure 7A). In seeking a method to predict mutation levels of oocytes, mean heteroplasmy levels in the blood of sibling children highly correlated with oocyte levels (Brown DT *et al*, *Am J Hum Genet* 68, 533-536 (2001); incorporated by reference herein) (R^2 = 0.52 vs. 0.85, Figure 7B).

Next, whole mtDNA sequences were analyzed in carrier oocytes in an effort to screen for secondary mtDNA mutations. Comparisons were made to oocytes from healthy donors. Carrier oocytes contained secondary heteroplasmic mtDNA variants, however the average number per oocyte was not significantly different from healthy controls (2.2 vs. 1.3; $p>0.05$) (Figure 7C). Some of these variants were present in several oocytes from the same carrier and were also found in the carrier's blood, skin or in sibling children suggesting recurring germline mutations. However, these variants were non-coding D-loop mutations. Others were found only in one oocyte within the group indicative of *de novo* mutations (45%). The majority (83%) of these secondary variants were low level heteroplasmic (<15%) mutations (Figure 11I). MtDNA copy number per oocyte was used as an indirect measure of oocyte quality (Monnot S *et al*, *Hum Mol Genet* 22, 1867-1872 (2013) and Fragouli E *et al*, *PLoS Genet* 11, e1005241 (2015); both of which are incorporated by reference herein). No significant differences between healthy and carrier oocytes (mean 348,954 vs. 283,605, respectively) were observed (Figure 7D). A low mtDNA copy number may play a role in diminished ovarian reserve (Boucret L *et al*, *Hum Reprod* 30, 1653-1664 (2015); incorporated by reference herein) but no correlation between oocyte copy number and AMH levels was observed herein. (Figure 11J).

In conclusion, carrier oocytes were of normal quality and the mutations levels in blood of sibling children seem to be of predictive value for mutation in oocyte cohorts.

Example 10 - Spindle transfer (ST) in mtDNA mutation carrier oocytes

Meiotic spindles (karyoplasts; with carryover maternal mtDNA) recovered from carrier MII oocytes (n=13) were transferred to enucleated donor oocytes (cytoplasts; donor mtDNA) (Figure 8A) while controls involved ST between healthy oocytes (n=36) with preselected mtDNA haplotypes (Figure 12A). All karyoplasts and cytoplasts survived micromanipulations and fusion except for one in the control group. ST oocytes along with intact (non-manipulated) controls were then fertilized by intracytoplasmic sperm injection (ICSI) and cultured to blastocysts. High fertilization rates, comparable to intact controls, were observed in both ST groups (Figure 8A and Figures 12B and 12C). Subsequent development of diploid carrier ST zygotes to the blastocyst stage was 75%, similar to controls. A similar developmental pattern was observed among carrier ST individuals with different mutation types (8993ST, 13513ST and 3243ST) (Figure 8B).

To address COS asynchrony, ideally both carriers and healthy donors would undergo same-day retrievals with the end point of a similar number of mature oocytes for ST. An alternative approach to achieve these objectives involves oocyte freezing, storage and thawing. ST between fresh and vitrified oocytes (frozen ST) was conducted. The overall fertilization rate using vitrified oocytes was comparable to fresh ST, while formation of normal diploid zygotes was lower (Figure 8A). No differences in fertilization were noted between karyoplast versus cytoplast vitrification (Figure 12D).

Since risk of miscommunication between nuclear and mitochondrial genomes has led to concerns regarding the potential secondary metabolic dysfunction (Woodson JD & Chory J, *Nat Rev Genet* 9, 383-395 (2008); incorporated by reference herein), ST embryo development was analyzed as a function of donor mtDNA sequence distance. ST oocytes and embryos were grouped based on the number of single nucleotide polymorphisms (SNPs) between the original (maternal) and donor oocyte mtDNA, ranging from the close (6 SNPs) to middle (33 SNPs) and to distant (57 SNPs) (Figure 12A). Fertilization and blastulation rates were similar among all three ST groups suggesting that embryo development is not compromised (Figure 8C). ESC lines were established from ST blastocysts and differentiated into neural progenitor cells (NPCs)

cardiomyocytes, and teratomas. Comparable differentiation efficiencies were observed between mitochondrial respiratory chain (RC) enzyme activity and oxygen consumption rates (OCR) among ESC derivatives carrying 6 or 49 SNP differences (Figures 8D, 13A, 13B, 16A, and 16B). Interestingly, differentiated cells from an ST-ESC line with 33 SNP differences displayed significantly reduced OCR levels, alluding possible nuclear to mitochondrial incompatibility.

In summary, MRT in carrier oocytes by ST resulted in high fertilization and blastocyst development similar to controls. In addition, embryo development, ESC derivation and differentiation were not affected by donor mtDNA genetic background. However, it is possible that certain donor mtDNA may not function properly, a process that was independent of total SNP differences.

Example 11 - Nuclear genome abnormalities

Because ST embryos may be at risk for chromosomal or sub-chromosomal abnormalities, expanded blastocysts derived from ST and control embryos were biopsied and examined by array CGH (comparative genome hybridization). A slightly higher aneuploidy rate was observed in both ST groups relative to intact controls but the difference was not significant. This could be related to older maternal age in the carrier group (Figures 14A and 17). Next, G-banding karyotype analysis was performed in ST and control ESCs. Abnormal karyotypes were observed in all groups but no significant differences were found. G-banding also detected cases of chromosomal mosaicism and polyploidy (Figures 14B and 18). Thus, to detect chromosomal abnormalities preimplantation genetic diagnosis can be performed prior to MRT embryo transfer.

Copy number variations (CNVs) were examined in selected ST-ES cell lines to explore possible subchromosomal abnormalities (deletion or duplications) (Lupski JR, *Trends Genet* 14, 417-422 (1998) and Sharp AJ *et al*, *Nat Genet* 38, 1038-1042 (2006); both of which are incorporated by reference herein). *De novo* CNVs were detected in both ST and intact controls but were deemed of uncertain clinical significance (Kearny HM *et al*, *Genet Med* 13, 680-685 (2011); incorporated by reference herein).

In summary, a total of 6 ST blastocysts were produced from 4 ovarian stimulation cycles in carriers (Table 4). One blastocyst was aneuploid and four were eligible for transfer based on morphological quality assessments. These outcomes were comparable to controls.

Table 4. MRT outcomes for families with pathogenic mtDNA mutations

	Family 1	Family 2	Family 3		Family 4	Family 5			
Mitochondrial disease	LS	LS	LS		LS	MELAS			
Pathogenic mtDNA mutation	T8993G	T8993G	G13513A		No	A3243G			
Age of carrier (yr)	22	23	36		28	32			
COS	Yes	Yes	Yes		Excluded	Yes			
No. retrieved oocytes	3	5	4		n/a	11			
No. ST oocytes	2	Canceled	4		n/a	7			
ST blastocysts	0	n/a	2		n/a	4			
Grade at D6	n/a	n/a	**5AA**	**5BB**	n/a	**5AA**	**5AA**	**5BB**	**5CC**
Aneuploidy	n/a	n/a	Yes:+9	n/t	n/a	n/t	No	No	No
Sex	n/a	n/a	M	n/a	n/a	n/a	M	F	F
mtDNA carryover	n/a	n/a	< 1%	n/a	n/a	n/a	< 1%	< 1%	< 1%*

Six ST embryos derived from oocytes carrying pathogenic mtDNA mutations reached the blastocyst stage. At least 2 blastocysts were eligible for transfer. *, mtDNA in ESCs from this blastocyst reverted to original maternal mtDNA haplotype but was wild type (did not carry A3243G mutation). n/a, non-applicable; n/t, non-tested.

Example 12 - Maintenance of donor mtDNA in ST embryos and ESC lines

MRT efficacy and safety depends not only on the degree of maternal mtDNA initially cotransferred with the karyoplast, but also on its subsequent persistence and possible amplification in embryos. Recent studies observed that due to genetic drift, some MRT ESCs restored maternal mtDNA (Yamada M *et al*, *Cell Stem Cell* 18, 749-754 (2016) and Hyslop LA *et al, Nature* 534, 383-386 (2016); both of which are incorporated by reference herein). Clearly, a small amount of maternal mtDNA carryover is common during ST resulting in low heteroplasmy in human embryos and in nonhuman primate offspring (typically below 2%) (Paull D *et al*, *Nature* 493, 632-637 (2013); incorporated by reference herein). Here, all examined ST zygotes and cleaving embryos (n=22) contained >99% donor mtDNA (Table 5) and similar outcomes were observed in 13 of 15 ES cell lines (87%) established from control ST blastocysts, regardless

of donor mtDNA haplotype. However, 2 ESC lines from sibling ST embryos (ST-ES7 and ST-ES8), generated by combination of maternal U5a and donor H1b mtDNA (33 SNPs), displayed high levels of maternal mtDNA (81% and 94%) (Table 5). Extended passaging resulted in a complete loss of the donor mtDNA and return to the original maternal mtDNA haplotype (100%).

Interestingly, two other genetically related ESC lines (ST-ES5 and ST-ES6) derived by reciprocal combination of maternal H1b and donor U5a showed high maintenance of donor mtDNA (>99%). Another ESC line generated from maternal U5a and donor V3 mtDNA (ST-ES9; 33 SNPs) also carried predominantly donor mtDNA.

Table 5. Donor mtDNA in human preimplantation MRT embryos and ESC lines

Treatment	Carryover maternal mtDNA %					Maternal haplotype	Donor haplotype	SNPs differences		
	Preimplantation Embryos		ESCs					Total	#Coding	D-loop
	Embryo stage	%	Lines	p.2-3	p.9-10					
Control ST	n/t		ST-ES1*	≤1	≤1	H56	H2a	6	4	1
	n/t		ST-ES2*	≤1	≤1	H2a	H56			
			ST-ES3	≤1	≤1					
	n/t		ST-ES4*	≤1	≤1	H44a	H13a	25	7	10
	n/t		ST-ES5	≤1	≤1	H1b	U5a	33	11	9
			ST-ES6	≤1	≤1					
	4-cell	0.7	ST-ES7	81±9	100	U5a	H1b			
	8-cell	0.9								
	10-cell	0.4	ST-ES8	94±4	100					
	10-cell	0.4								
	1-cell	0.4	ST-ES9	≤1	≤1	U5a	V3	33	11	9
	2-cell	0.5								
	8-cell	0.5								
	Morula	0.4	ST-ES10	≤1	≤1	V3	U5a			
	1-cell	0.5*	ST-ES11*	≤1	≤1	H1e	D1f	44	15	14
	n/a	0.9*	ST-ES12*	≤1	≤1					
		1.6*								
		0.0*	ST-ES13*	≤1	≤1					
	1-cell	0.5	ST-ES14	≤1	≤1	D4a	A2g	49	18	16
	Morula	0.2								
	Morula	0.2								
	1-cell	0.2								
	1-cell	0.5	ST-ES15	≤1	≤1	A2g	D4a			
	1-cell	0.5								
	1-cell	0.5								
Carrier ST	1-cell	0.8	n/a			H1b	H6a	20	5	11
	3-cell	0.5								
	3-cell	0.6								
	n/t		13513ST-ES	≤1	≤1	T2b	T2	22	3	5
	1-cell	0.5	3243ST-ES1	20±13	100	H49	B2k	32	7	14
	8-cell	0.8								
	12-cell	0.5	3243ST-ES2	≤1	≤1					
	Morula	0.5								
SCNT	n/t		NT-ES1		≤1	H1b	H56	13	5	7
			NT-ES2		≤1					
			NT-ES3		≤1					
			NT-ES4		≤1					
			NT-ES5		≤1	F1a	D1a	47	16	11
			NT-ES6		≤1	F1a	H1b	38	13	13
			NT-ES7	≤1	≤1	X2c	U5a	40	9	16
			NT-ES8	19±9	100	X2c	D4a	39	12	13

Among the three carrier ST-ESC lines, 3243ST-ES1 also contained a significant level of maternal mtDNA (20%) (Table 5). However, this maternal H49 haplotype did not include the A3243G mutation. Maternal mtDNA levels in this cell line gradually increased during extended culture to 90% at passage 8 and to homoplasmy at p.10 (Figure 9A). Remarkably, another

sibling ESC line (3243ST-ES2) generated by the same maternal and donor mtDNA combination did not show any increase in maternal mtDNA, presumably due to stochastic or bottleneck effects (Table 5).

The study was expanded to include eight ESC lines derived by SCNT (NT-ESCs) that also carry donor oocyte mtDNA (Table 5) (Tachibana M *et al*, *Cell* 153, 1228-1238 (2013); Ma H *et al*, *Nature* 524, 234-238 (2015); and Kang E *et al*, *Cell Stem Cell* 18, 625-636 (2016); incorporated by reference herein). MtDNA heteroplasmy dynamics were analyzed during extended passaging and identified that NT-ES8 displayed a gradual increase of maternal (somatic) mtDNA from 19% at p. 2 to 100% at p.10 (Table 5, Figure 15A). Note that this NT-ESC line was generated by combination of maternal X2c and donor D4a mtDNA haplotypes (39 SNPs).

In conclusion, ST allows efficient replacement of oocyte mtDNA with very low carryover mtDNA in the resulting preimplantation embryos. The majority of ESCs derived from ST blastocysts maintained predominantly donor mtDNA. However, some ESC lines displayed gradual loss of the donor and reversion to the maternal mtDNA, requiring further research to better understand underlying mechanisms.

Example 13 - Molecular and cellular mechanisms contributing to maintenance of donor mtDNA

Based on the observation that specific haplotype combinations led to reversal to the maternal mtDNA, it was hypothesized that this could be due to preferential replication of specific mtDNA haplotypes or that certain mtDNA endow cells with growth advantages (Burgstaller JP *et al*, *Mol Hum Reprod* 21, 11-22 (2015) and Agaronyan K *et al*, *Science* 347, 548-551 (2015); both of which are incorporated by reference herein).

The highly polymorphic mtDNA D-loop region, called conserved sequence box II (CSBII) was focused on first. It has been previously shown that a rare polymorphism in the CSBII, namely G5AG7, affects efficiency of mitochondrial transcription termination and replication primer generation. When the donor and maternal mtDNA were compared in a total of 26 ESC lines with 18 different haplotype combinations it was observed that two “reversed” sibling ST-ES7 and ST-ES8 carried donor mtDNA with a G5AG8 polymorphism while the maternal mtDNA

was G6AG8. Using *in vitro* transcription assays it was determined whether synthesis of the replication primer by mitochondrial RNA polymerase was affected in donor mtDNA. It was found that the deletion of a single guanosine residue (G5AG8 vs. G6AG8) in donor mtDNA results in a 4-fold reduction of replication primer synthesis (Figure 9a). Therefore, certain mtDNA haplotypes varying in the CSBII sequence provide more efficient synthesis of the replication primer and, subsequently, may achieve replicative advantage. Without being bound by theory, this mechanism could explain the phenomenon of preferential replication of maternal mtDNA in some of the ESC lines. Sequence analysis did not find CSBII SNP differences in the remaining two reversed 3243ST-ES1 and NT-ES8. A number of other D-loop polymorphisms were observed including the core TAS region, which is also implicated in regulation of mtDNA replication (Jemt E *et al*, *Nucl Acids Res* 43, 9262-9275 (2015); incorporated by reference herein). Although the exact mechanism by which these polymorphisms affect replication remain unclear, it can be speculated that, similar to the CSBII and TAS regions, some D-loop variants may result in replication bias of a particular mtDNA haplotype.

It was also considered if additional replication-independent mechanisms affect the reversal to maternal mtDNA and examined the increase in maternal mtDNA in reversed 3243ST-ES1 and NT-ES8 in whole cultures or individual cell clones. Starting maternal mtDNA levels increased with passaging in whole cultures (Figures 9B, 9C, and 15A). However, when ESCs were disassociated into individual cells and cultured isolated single cell clones, the starting maternal mtDNA levels varied in different clones but the heteroplasmy did not change with extended culture (Figure 9D). Significant differences in cell proliferation and growth rates among different clones were observed. Clones with higher maternal mtDNA levels exhibited significantly faster growth rates than clones with lower maternal mtDNA heteroplasmy (Figure 9E). These results suggest that certain mtDNA haplotypes confer ESCs with faster growth and proliferative advantages. Thus, in mixed cultures consisting of cells with varying heteroplasmy, a sub-population of cells with higher maternal mtDNA may overgrow cells with donor mtDNA.

Mitochondrial respiratory chain complex I and complex IV enzyme activities were measured in cells carrying various mtDNA haplotypes but no significant differences were found. This suggests that the reversal to maternal mtDNA is independent of mitochondrial activity (Figure 15B).

Next, it was examined if the reversal is specific to undifferentiated ESCs or could occur during differentiation. Several reversed and non-reversed ESCs were differentiated in *vitro* into NPCs and cardiomyocytes, and *in vivo* into teratomas. Maternal mtDNA levels were measured before and after differentiation (Figures 16A, 16B). Maternal mtDNA levels in the reversed 3243ST-ES1 reduced to undetectable levels in some tissues but were slightly elevated in other cell types compared to the initial 4% in undifferentiated ESCs (Figure 9F). The maternal mtDNA was undetectable during *in vivo* and *in vitro* differentiation of the nonreversed sibling cell line 3243ST-ES2. In contrast, maternal mtDNA levels increased in all tested differentiated tissues in the reversed ST-ES7 and NT-ES8 (Figure 9F). These results demonstrate that the mtDNA reversion phenomenon is not unique to ESCs and occurs during differentiation, raising the possibility that return to the mutant mtDNA may occur in some MRT children.

Example 14 – Conclusions

The feasibility and clinical outcomes following MRT in oocytes carrying pathogenic mtDNA mutations was investigated 8, 10. Since mutations in either nuclear or mtDNA genes can cause similar mitochondrial syndromes, it is critical to conduct genetic testing to confirm the eligibility of women with pathogenic DNA mutations for MRT.

A range of heteroplasmy for mutant mtDNA was observed among different tested tissues in women carriers and their children. As expected, pathogenic mtDNA mutations were detected in oocytes from all carriers.

Carryover of the maternal mtDNA, while detectable, was below 1% in preimplantation ST embryos. However, reversion to the original maternal mtDNA was observed in a few MRT ESCs (15%, 4/26) during their extended culture or differentiation. Maternal mtDNA in ST monkeys was at expected low levels and did not increase with age in adults. However, a moderate increase in maternal mtDNA (16%) was seen in selected oocytes from ST females (Lee

HS *et al*, *Cell Rep* 1, 506-515 (2012); incorporated by reference herein). This implies that despite efficient replacement of the mutant mtDNA in oocytes, some MRT children may still develop high mutation loads and mitochondrial disease.

Among the factors that might contribute to the mtDNA reversion, it appears that this phenomenon was irrespective of MRT methods (ST, PNT or SCNT), presence of pathogenic mtDNA mutations and the genetic distance measured in total SNPs between donor and maternal mtDNA. However, some specific haplotype combinations produced preferential increase of the maternal and gradual loss of the donor mtDNA. One of the possible mechanisms responsible for the observed reversal could be more efficient replication primer synthesis and thus bias towards preferential amplification of mtDNA haplotypes with specific CSBII sequence polymorphisms. The selection of compatible donor mtDNA harboring CSBII or other D-loop sequences similar to the maternal mtDNA would solve this problem. While the number of tested combinations in the disclosed study is small, the possible order of replication advantage in mtDNA haplotypes could be H56 > H1b, U5a > H1b > F1a, U5a >X2c > D4a and H49 > B2k. However, stochastic or bottleneck mtDNA amplification during early embryo development may also coexist.

Mitochondria not only generate energy but also regulate cell proliferation and apoptosis (Chan DC *et al*, *Cell* 125, 1241-1252 (2006); incorporated by reference herein). Disclosed herein are mtDNA haplotypes could affect cell growth and proliferation thus providing selective advantage for cells with maternal mtDNA. Future applications of MRT will require additional studies evaluating compatible donor mtDNA haplotypes to avoid OXPHOS dysfunction, differences in mtDNA replication, cell growth and recovery of mutant mtDNA (Koehler CM *et al*, *Genetics* 129, 247-255 (1991); incorporated by reference herein).

Example 15 – mtDNA sequencing

Specific mtDNA mutations and general haplotypes were determined in oocytes, blood, skin fibroblasts (SF) and/or urine by whole mtDNA sequencing using MiSeq or amplification refractory mutation system-quantitative polymerase chain reaction (ARMS-qPCR).

Example 16 - Controlled ovarian stimulation (COS)

Baseline screening was conducted including a medical history and physical exam, assessment of body mass index (BMI), anti-mullerian hormone (AMH) level, and antral follicle count (AFC). Subjects underwent ovarian stimulation and oocyte retrieval employing standard IVF protocols and procedures.

Example 17 - Spindle transfer (ST)

ST was performed as follows: meiotic metaphase II (MII) spindles were visualized under polarized microscopy and isolated with minimal cytoplasm (karyoplast, host mtDNA). The karyoplast was then placed in the perivitelline space of an enucleated oocyte (cytoplast, donor mtDNA) and fused using HVJ-E (hemagglutinating virus of Japan-envelope).

Example 18 - Oocyte vitrification

Oocyte vitrification was performed as previously described using commercially available human oocyte vitrification & thawing kits (Vitrification kit and Vit. Warming kit, Life Global).

Example 19 - Derivation of ES cells and culture

ST blastocysts were freed from their zonae pellucidae and plated on mEF feeder layers on 4-well culture dishes for 5-7 days at 37°C, 3% CO_2, 5% O_2, and 92% N_2 in medium (DMEM/F12 with 10% FBS, 10% KSR, 0.1 mM nonessential amino acids, 1 mM l-glutamine, 0.1 mM β-mercaptoethanol, 5 ng/ml basic fibroblast growth factor, 10μM ROCK inhibitor). Attached blastocyst outgrowths were manually minced into small pieces, re-plated onto fresh plates and maintained in knockout DMEM medium (Invitrogen) supplemented with 20% KSR, 0.1 mM nonessential amino acids, 1 mM l-glutamine, 0.1 mM β- mercaptoethanol, penicillin-streptomycin and 4 ng/ml bFGF for further propagation and analysis. All cell lines were negative for mycoplasma contamination.

Example 20 - mtDNA transcription assays *In vitro* transcription anti-termination assays were performed using PCR-amplified templates containing region 202-481 of donor (H1b or host (U5a) mtDNA. The products of the transcription reactions were resolved by 20% PAGE containing 6 M urea and visualized by PhosphoImager (GE Health).

Example 21 - Cell growth and proliferation assays

ESCs were adapted to grow under feeder-free conditions on Matrigel matrix in mTeSRTM1 medium (STEMCELL technologies) (Wu J *et al*, *Nature* 521, 316-321 (2015); incorporated by reference herein). The cells were dissociated with Accutase (Life Technologies) for 2 min and approximately 10^5 cells were seeded into each 60 mm dish. The cells were harvested were periodically harvested and counted using Countess Automated Cell Counter (Invitrogen).

Example 22 - Neural progenitor cells (NPC) differentiation and culture

A previously published protocol with minor modifications was used for NPC differentiation. Briefly, ESCs were maintained on MEFs in CDF12 medium before NPC differentiation. CDF12 medium contained DMEM/F12 (Life Technology), 20% knockout serum replacement (Life Technologies), 2 mM Glutamax (Life Technologies), 0.1 mM NEAA (Life Technology), 0.1 mM β-mercaptoethanol (Life Technologies) and 4 ng/ml FGF2 (Peprotech). ESCs were disaggregated with Collagenase IV (Life Technologies) and allowed to grow to about 40% confluence. To initiate neural induction, cells were washed twice with DPBS 1x without calcium & magnesium (Corning Cellgro) and changed to Neural Induction Medium 1 (NIM-1: 50% Advanced DMEM/F12 (Invitrogen), 50% Neurobasal (Invitrogen), 1x B27 (Invitrogen), 1x N2 (Invitrogen), 2 mM GlutaMAX and 10 ng/ml hLIF (Peprotech), 4uM CHIR99021 (Selleckchem), 3 uM SB431542 (Selleckchem), 2 uM Dorsomorphin (Sigma), and 0.1 uM Compound E (EMD Chemicals Inc.). After 2 days culture in in NIM-1 medium, cells were switched to Neural Induction Medium 2 (NIM-2: 50% Advanced DMEM/F12, 50% Neurobasal, 1x N2, 1x B27, 2 mM GlutaMAX and 10 ng/ml hLIF, 4uM CHIR99021, 3 uM SB431542 and 0.1 uM Compound E). Cells were further cultured in NIM-2 for 5 days with daily medium change. At the last day in NIM-2 medium, cells were treated overnight with 10uM Y27632 (Selleckchem) and 20-30 "dome"-shaped colonies were manually picked and digested with Accumax (Innovative Cell Technologies) for 10 minutes at 37°C. After Accumax treatment cells were gently disaggregated into single cells and re-plated onto Matrigel-coated 6-well plates at a density of about 3.5 x 10^4 per cm^2 in Neural Progenitor cell Maintenance Medium (NPMM: 50% Advanced DMEM/F12, 50% Neurobasal, 1x B27, 1x N_2, 2 mM GlutaMAX, 10ng/ml hLIF, 3 uM CHIR99021 and 2uM

SB431542) supplemented with 10 uM Y27632. NPCs were maintained on Matrigel-coated dishes in NPMM. NPCs were passaged when reached around 70% to 80% confluence using Accumax and replated at a density of 3 x 10^4 per cm^2 with daily medium change. For the initial 6 passages, NPCs were pre-treated with 10 μM Y27632 overnight before and during cell splitting. The study was randomized, and the investigators were blinded to treatment allocations in collaborators' laboratories.

Example 23 - Cardiomyocyte differentiation

Cardiomyocyte differentiation was performed based on a GiWi (GSK3 inhibitor and Wnt inhibitor) protocol described previously (Lian X *et al*, Nat Protoc 7, 1235-1246 (2012); incorporated by reference herein). Briefly, ESCs were grown on Matrigel-coated plates in mTeSR1 medium to 80-90% confluence before passaging with Accutase and then re-seeded at 0.5-1.5 million cells per well in 12-well plates in 1 ml of mTeSR1 plus 10 μM Y27632. On day 5, cells were incubated with 6 to 12 μM CHIR99021 (Selleckchem) for 16-24 h and then medium replaced with 2ml of RPMI/B27 (-insulin) and cultured for two days. On day 8, a 2 ml combined medium was prepared by mixing 1ml medium collected from the 12-well plate and 1ml fresh RPMI/B27 (-insulin) medium. Cells were then replaced with 2ml combined medium with 5 μM IWP2 (Tocris) added and cultured for 48 h. At day 10, 2 ml of fresh RPMI/B27 (-insulin) was added to each well of the 12-well plate. Starting from day 12 medium was changed every three days with 2 ml/well of RMPI/B27 (+insulin). Contracting cardiomyocytes were observed as early as day 17 from the initial passaging of ESCs. Differentiated cell types were identified by immunocytochemistry as described previously.

Example 24 - Teratoma assay

ESCs were injected into the femoral region of 6-week-old, SCID male mice (Charles River). Mice with tumors were euthanized and teratomas were isolated, sectioned and histologically characterized for the presence of representative tissues as described previously.

Example 25 - Assessment of mitochondrial function

Mitochondrial respiratory chain enzymatic activities (Complex I and IV) were measured by spectrophotometry, as described in, for example, Spinazzi M *et al*, *Nat Protoc* 7, 1235-1246

(2012); incorporated by reference herein. Briefly, intact mitochondria were isolated from fibroblasts and treated with and without 3 mM rotenone at a 340 nm wavelength for 5 min. Differences of absorbance per minute were obtained, and the specificity of COMI activity was estimated by the percentage of rotenone inhibition. For live cell oxygen consumption, a XF96 Extracellular Flux Analyzer (Seahorse Biosciences) was used to measure oxygen consumption rates (OCR) and extracellular acidification rates (ECAR) as described previously29. Briefly, neural progenitor cells (NPCs) were seeded at a density of 30,000 cells per well of a XF96 cell culture microplate and incubated for 24 h to allow cells to attach. Prior to assay, NPCs were equilibrated for 1 h in unbuffered XF assay medium supplemented with 25 mM glucose, 1 mM sodium pyruvate, 2 mM glutamax, 1x nonessential amino acids and 1% (v/v) FBS in a non-CO2 incubator. Sequential compound injections of oligomycin (0.5 µg/ml), carbonyl cyanide 4-(trifluoromethoxy) phenylhydrazone (FCCP, 1 µM) and rotenone (0.5 µM)/antimycin A (1 µM) were used to measure the key parameters of mitochondrial respiration. Indices of mitochondrial function were calculated as basal respiration rate (baseline OCR – rotenone/antimycin A OCR), ATP dependent (basal respiration rate – oligomycin OCAR), maximal respiration rate (FCCP OCR – rotenone/antimycin A OCR) and oxidative reserve (maximal respiration rate – basal respiration rate). Each plotted value was the mean of a minimum of 4 replicate wells, and was normalized to total cell numbers plated. Results were presented as means ± SEM. One-way ANOVA was used for three group comparisons and student's t test was used for pairwise comparisons. A P-value less than 0.05 was considered as significant. The study was randomized, and the investigators were blinded to sample allocations among different groups.

Example 26 - mtDNA sequencing by MiSeq

DNA was extracted from skin fibroblasts, whole blood, Urine, ESCs and teratoma tissues using Gentra DNA extraction kit (Qiagen), and from oocytes using Pico Pure DNA Extraction Kit (Life Technologies). mtDNA was amplified by a single PCR reaction. mtDNA amplification from individual oocytes was performed using 2 primer sets: 7272F 5-GGCTCATTCATTTCTCTAACAG-3,

15712R 5-TTGGCTTAGTGGGCGAAATA-3 and 15635F 5-TCCATCCTCATCCTAGCAAT-3, 7401R 5-GGGGGCATCCATATAGTCAC-3 and mitochondrial sequencing performed.

Example 27 - Detection of mtDNA variants by Sanger sequencing

mtDNA variants present at over 10% heteroplasmy were corroborated independently by Sanger sequencing. Regions of mtDNA containing germline mutations or SNPs were amplified by PCR with previously reported primer sets using PCR Platinum SuperMix high fidelity kit (Life Technologies . PCR products were purified, sequenced and analyzed by Sequencher v. 5.0 (GeneCodes).

Example 28 - ARMS-qPCR and copy number measurement

The amplification refractory mutation system quantitative PCR assay (ARMs-qPCR) was performed to verify heteroplasmy at mt8993T>G, mt13513G>A and mt3243A>G and to measure carryover in control ST embryos and ES cells at 7843A>G, 16519T>C and 16278T>C8. Measurement of mtDNA copy number was performed.

Example 29 - Genetic and cytogenetic analyses

Karyotyping by G-banding was performed on 20 metaphase cells from each human cell line. Array CGH was performed by IVI Gen. CNVs were identified by SNP genotyping as previously described in Ma H *et al*, *Nature* 511, 177-183 (2014) incorporated by reference herein and analyzed by a clinical genetic diagnosis laboratory.

Example 30 - Statistical analysis

Results are presented as means ± SD. or SEM. $p<0.05$ was considered significant. Data were analyzed using Pearson non-parametric test for correlation, independent group t-test or chi-square test for pairwise comparison and ANOVA with Bonferroni analysis for multiple comparisons (IBM SPSS).

CLAIMS

1. A method for preparing a viable human oocyte for fertilization, the method comprising the steps of:

a) isolating a first oocyte containing a polar body;
b) gaining access through the zona pellucida of the first oocyte;
c) removing the polar body from the first oocyte;
d) removing the nuclear spindle from a second oocyte to create an enucleated cytoplast;
e) placing the polar body removed from the first oocyte into the perivitelline space of the enucleated cytoplast.

2. The method of Claim 1 further comprising fertilizing the viable human oocyte via in vitro fertilization, thereby creating an embryo.

3. The method of Claim 2 further comprising implanting the embryo in a receptive uterus.

4. The method of any of Claims 1-3 where enucleating the first oocyte is performed in a medium comprising at least 10% human tubal fluid, HEPES buffer, and cytochalasin B using a Polarized Microscope Imaging System.

5. The method of any of Claims 1, 2, or 3 where isolating the polar body is performed in a medium comprising at least 10% human tubal fluid, HEPES buffer, cytochalasin B, and fusion with donor cytoplast induced with HVJ-E extract.

6. A method of producing a human oocyte in vitro, the method comprising:

a) determining a mitochondrial DNA sequence of the conserved sequence box II of a donor oocyte;

b) enucleating the donor oocyte while the donor oocyte is arrested at metaphase II, thereby isolating donor nuclear genetic material;

c) introducing the donor nuclear genetic material into an enucleated recipient oocyte, provided that the mitochondrial DNA of the donor oocyte has the same conserved sequence box II genotype as the recipient oocyte.

7. The method of claim 6 further comprising fertilizing the viable human oocyte via in vitro fertilization, thereby creating an embryo.

8. The method of claim 7 further comprising implanting the embryo in a receptive uterus.

9. The method of any of Claims 6, 7, or 8 where enucleating the donor oocyte is performed in a medium comprising at least 10% human tubal fluid, HEPES buffer, and cytochalasin B using a Polarized Microscope Imaging System.

10. The method of any of Claims 2, 3, 7, and 8, in which the embryo is cultured to the blastocyst stage prior to implantation in a receptive uterus.

11. The method of any of Claims 6, 7, 8, 9, or 10 where the donor oocyte and the recipient oocyte both have the G5A8 genotype or both have the G6A8 genotype.

12. The method of any of Claims 6, 7, 8, 9, or 10 where the mitochondrial DNA from the donor oocyte comprises a mutation that results in a mitochondrial disease.

13. The method of Claim 12 where the mitochondrial disease is selected from Leigh Syndrome and Mitochondrial Encephalomyopathy Lactic Acidosis and Stroke-like Episodes.

14. A method of producing a human oocyte in vitro, the produced human oocyte comprising minimal maternal mitochondrial DNA, the method comprising:

determining the sequence of the major non-coding region of the mitochondrial DNA of a donor oocyte, where the major non-coding region sequence includes a D loop region;

enucleating the donor oocyte while the donor oocyte is arrested at metaphase II, thereby isolating donor nuclear genetic material;

introducing the donor nuclear genetic material into an enucleated recipient oocyte, provided that the mitochondrial DNA of the donor oocyte has the same major non-coding region sequence as the recipient oocyte.

15. The method of Claim 14 where the donor oocyte and the recipient oocyte both have the H56, H1b, U5a, F1a, X2c, D4a, H49, or B2k mtDNA haplotype.

16. The method of Claim 14 where the mitochondrial DNA from the donor oocyte comprises a mutation that results in a mitochondrial disease.

17. The method of Claim 16 where the mitochondrial disease is Leigh Syndrome or Mitochondrial Encephalomyopathy Lactic Acidosis and Stroke-like Episodes.

Figure 1A

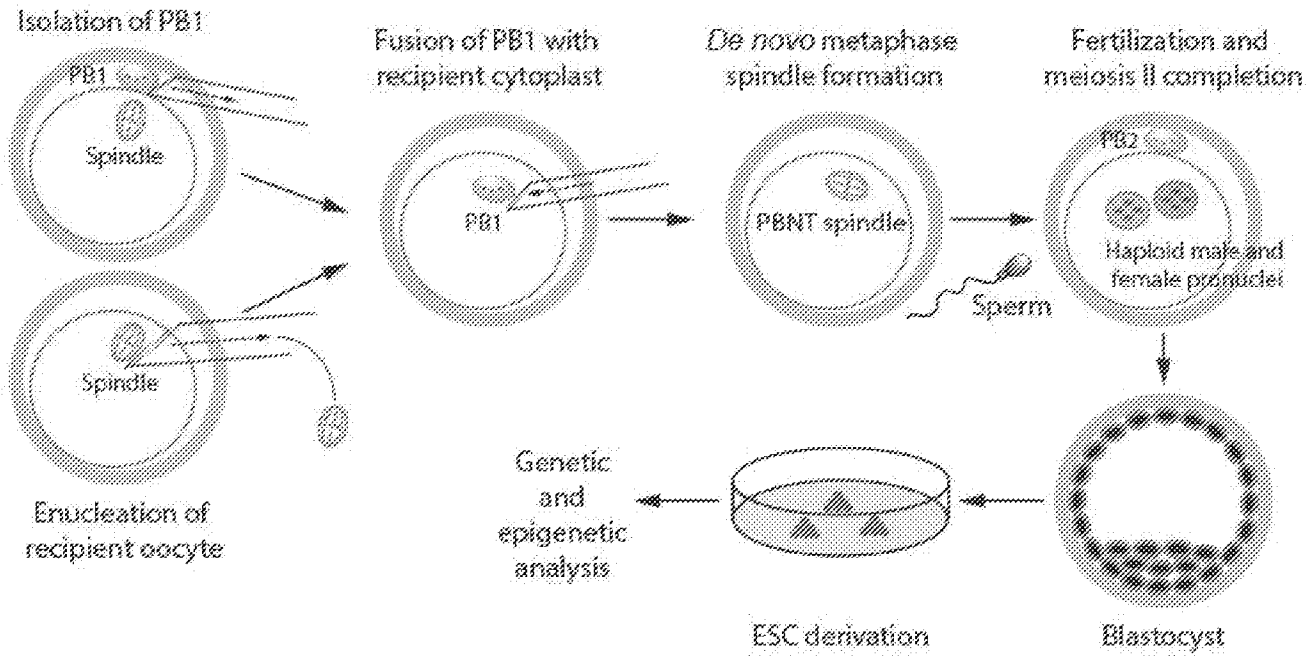


Figure 1B



Figure 1C

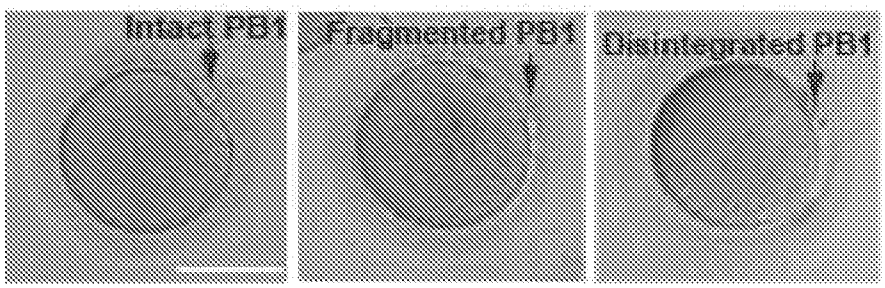


Figure 1D

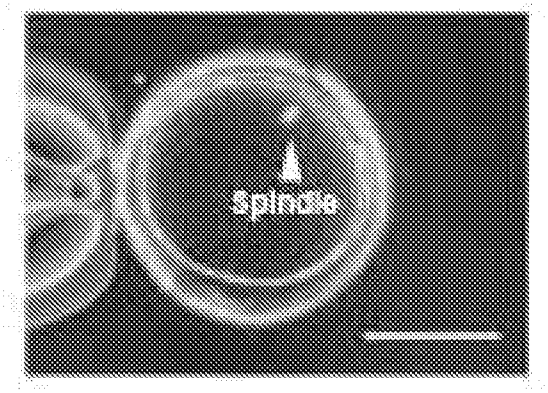


Figure 1E

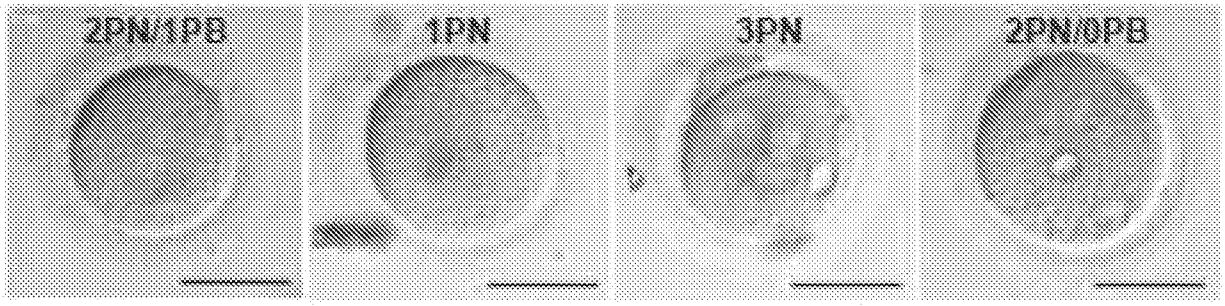


Figure 1F

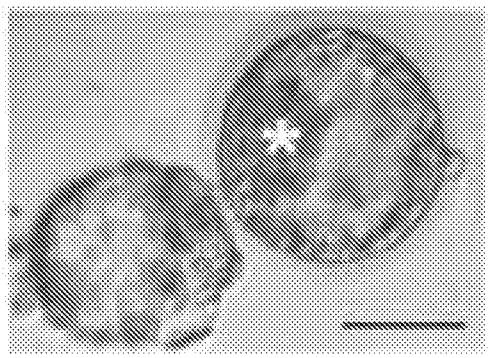


Figure 1G

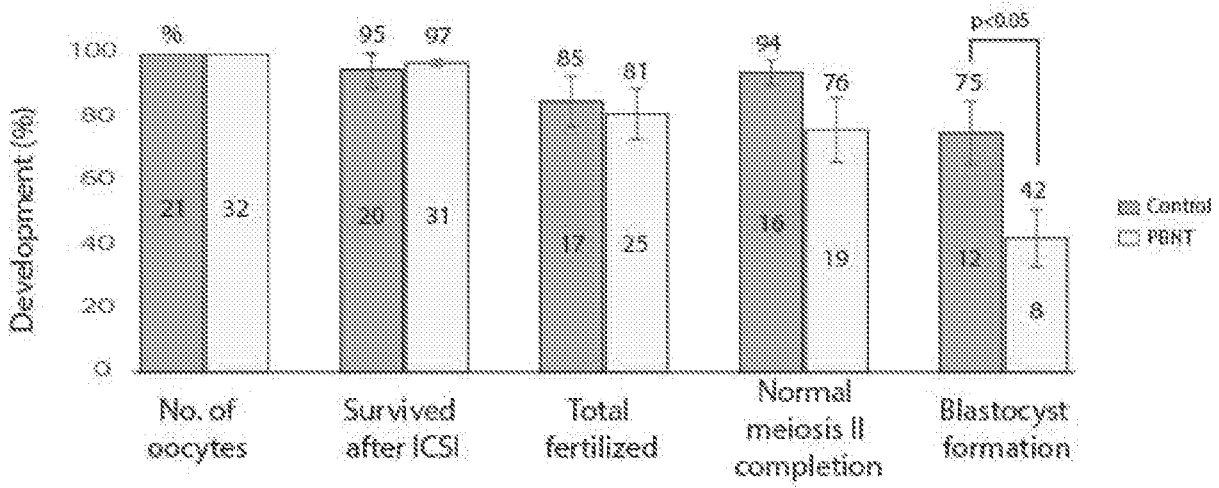


Figure 2A

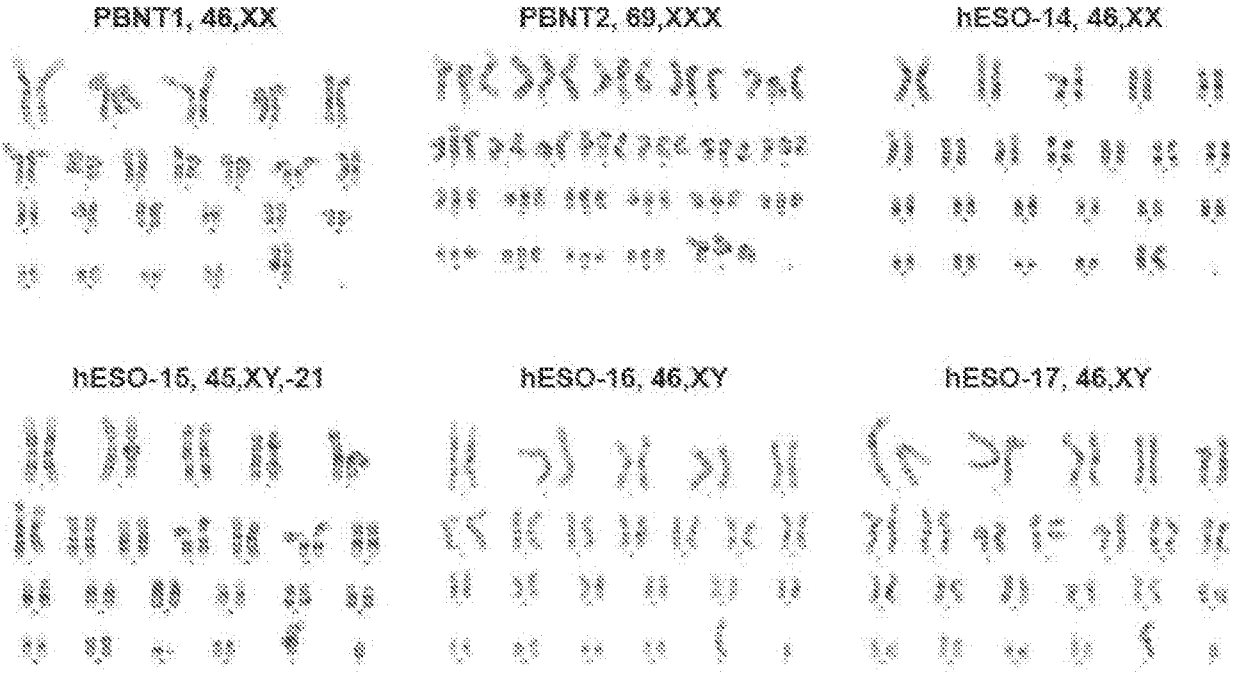


Figure 2B

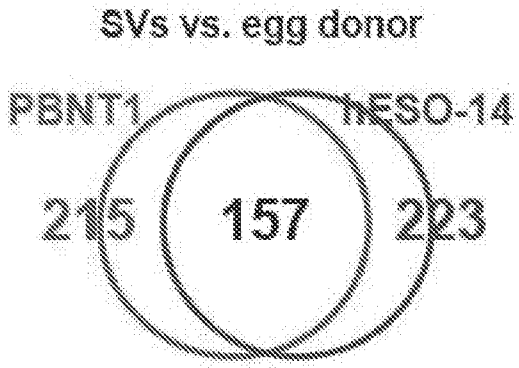


Figure 2C

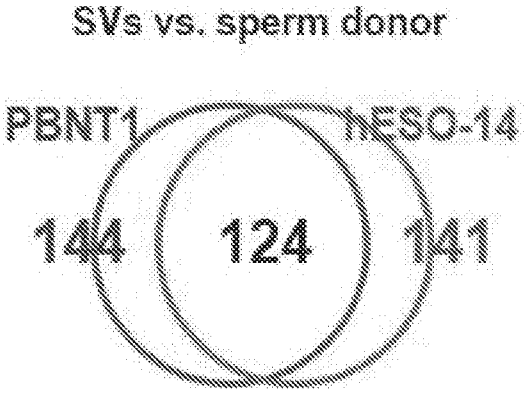


Figure 2D

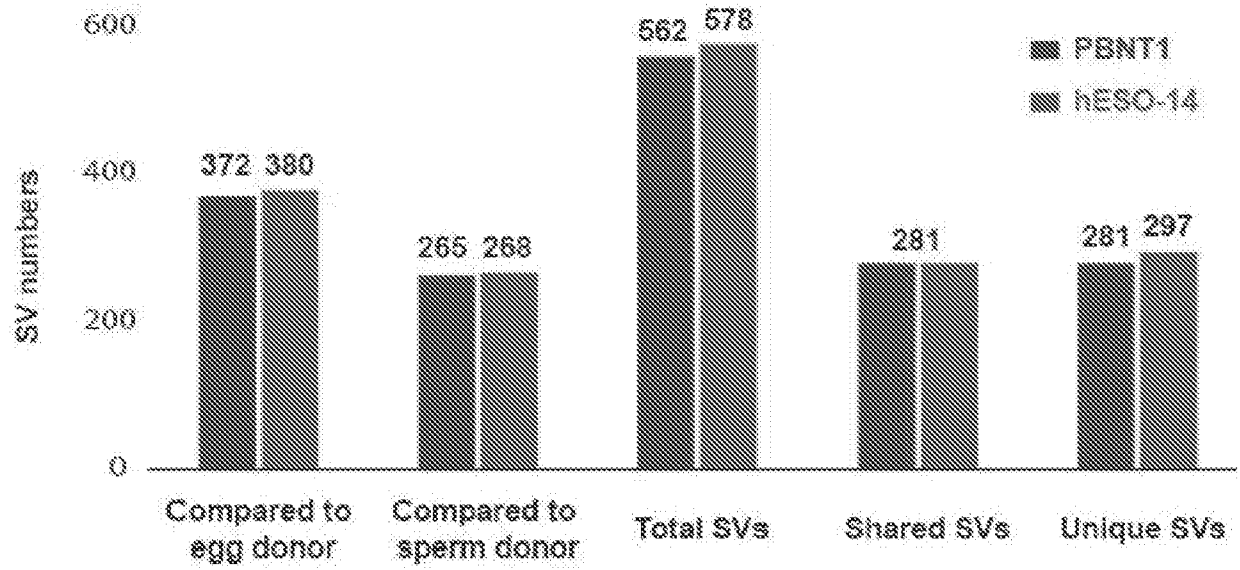


Figure 3A

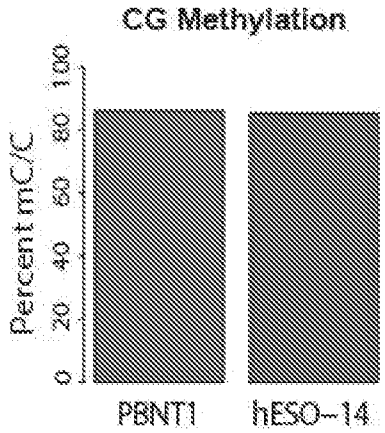


Figure 3B

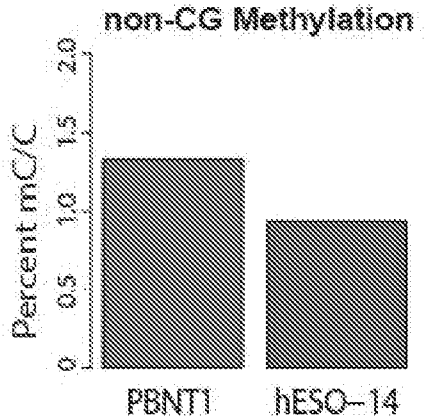
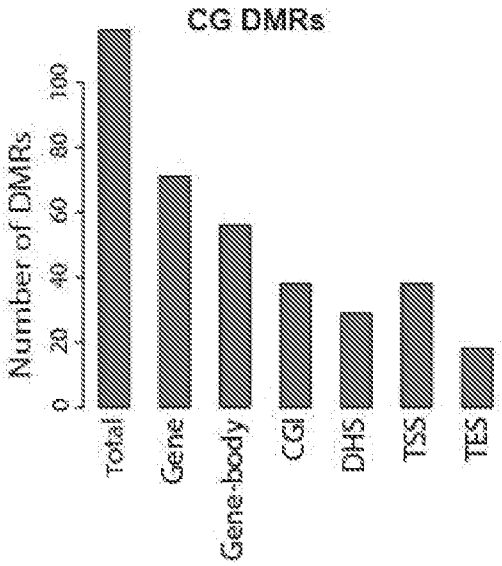


Figure 3C



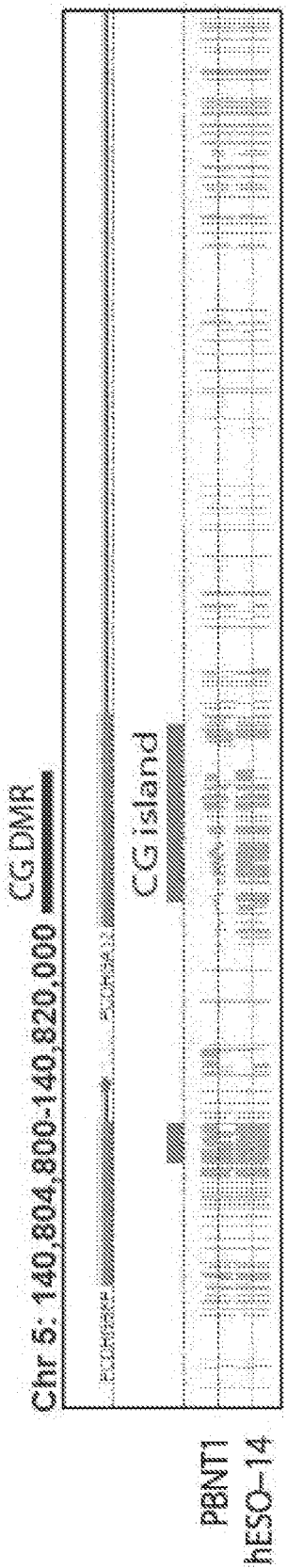


Figure 3D

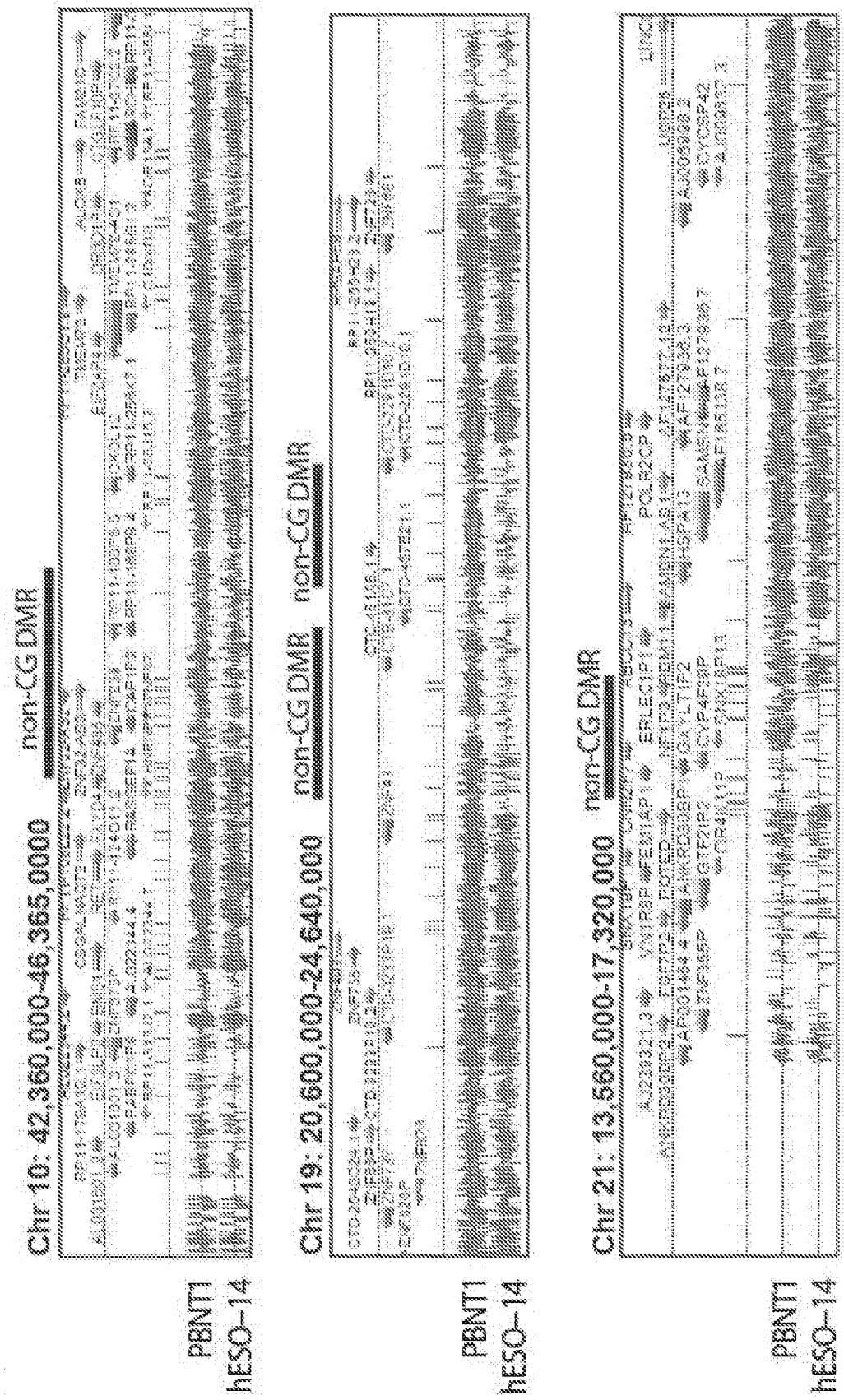

Chr 10: 42,360,000-46,365,0000
non-CG DMR
PBNT1
hESO-14
Chr 19: 20,600,000-24,640,000
non-CG DMR
non-CG DMR
PBNT1
hESO-14
Chr 21: 13,560,000-17,320,000
non-CG DMR
PBNT1
hESO-14

Figure 3E

Figure 4A

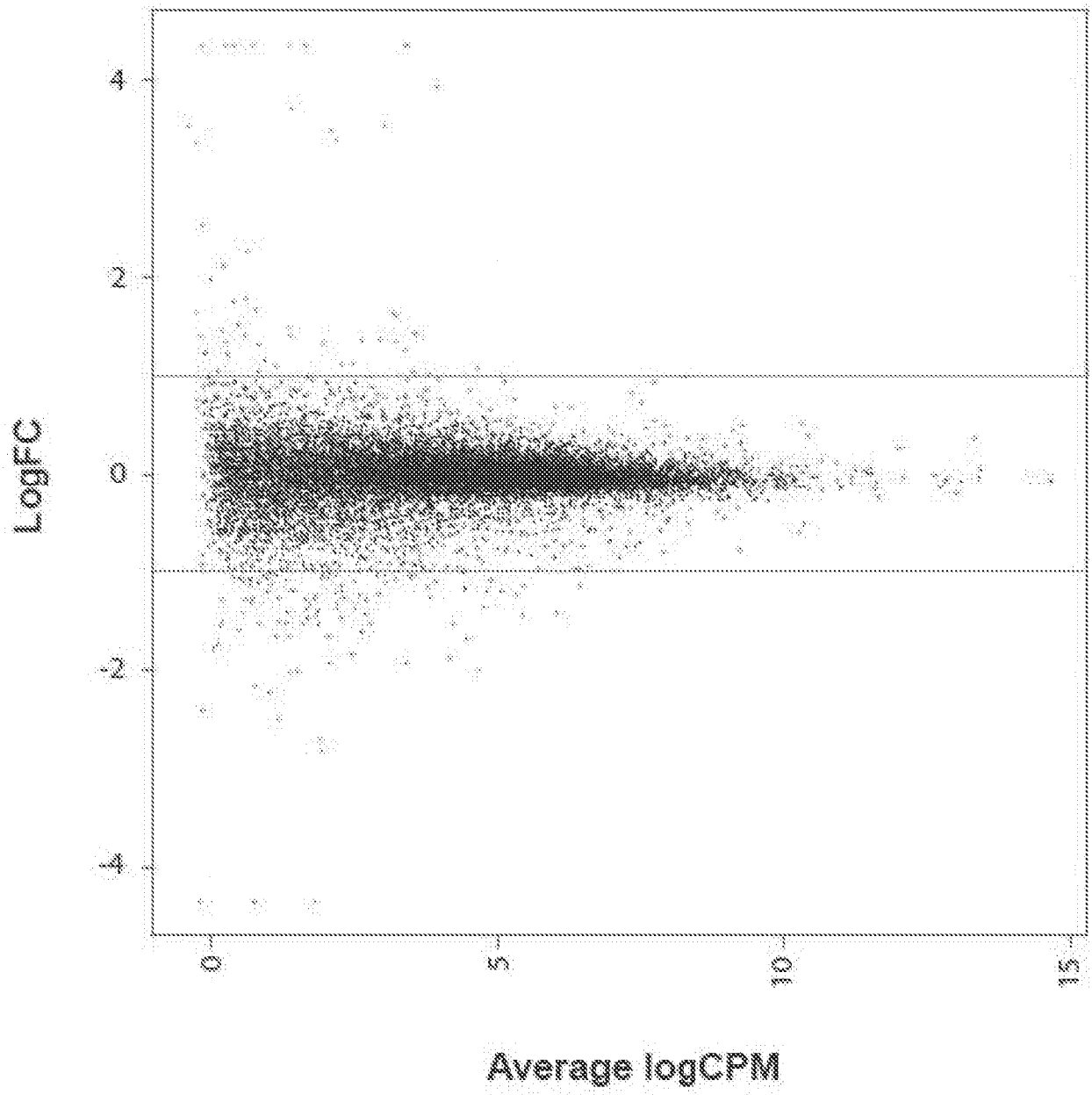


Figure 4B

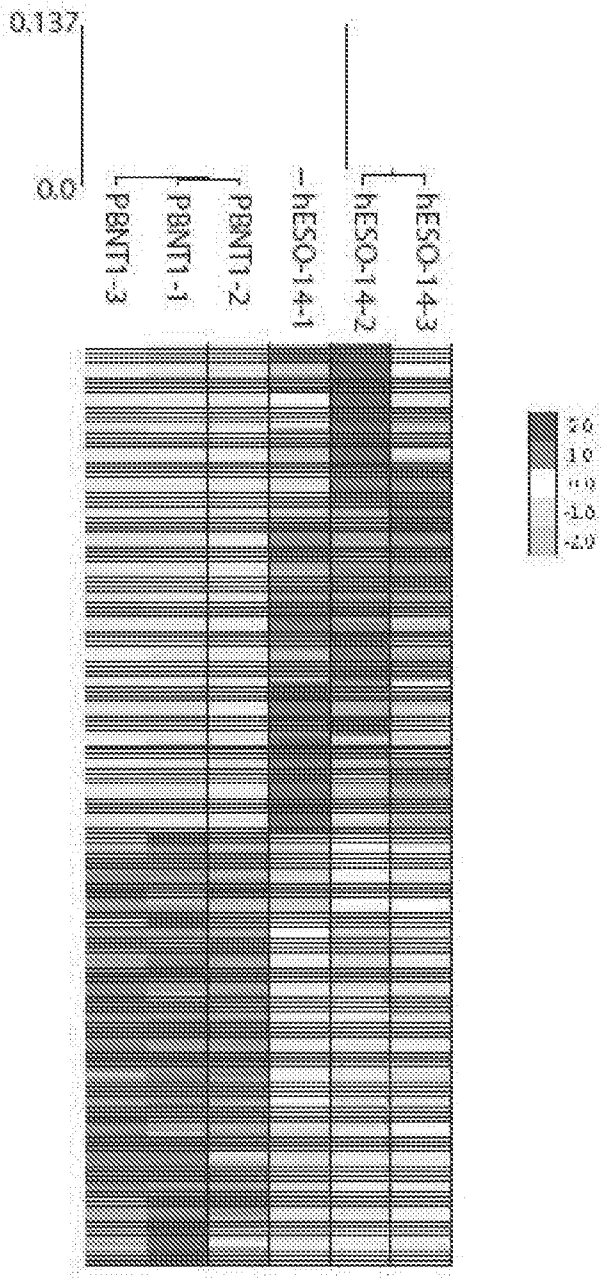

0.137
0.0
PBNT1-3
PBNT1-1
PBNT1-2
hESO-14-1
hESO-14-2
hESO-14-3
2.0
1.0
0.0
-1.0
-2.0

Figure 5A

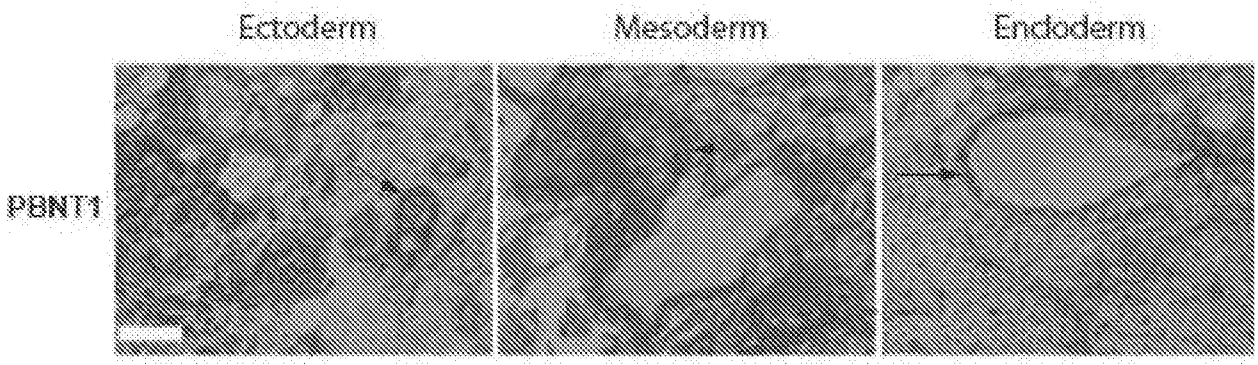


Figure 5B

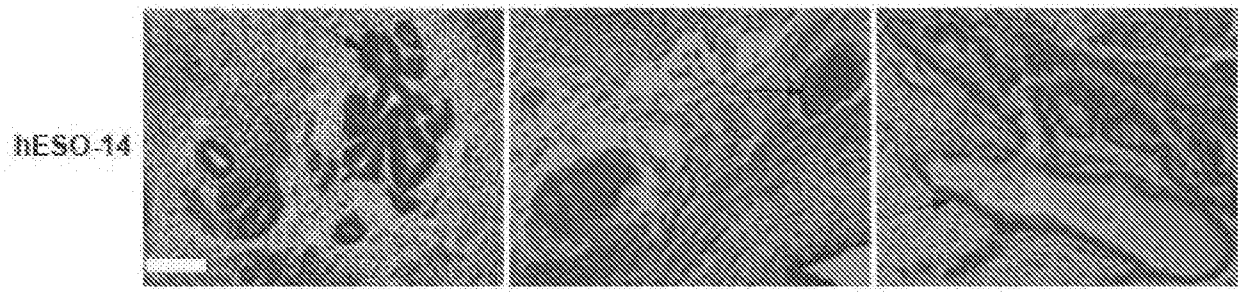


Figure 6A

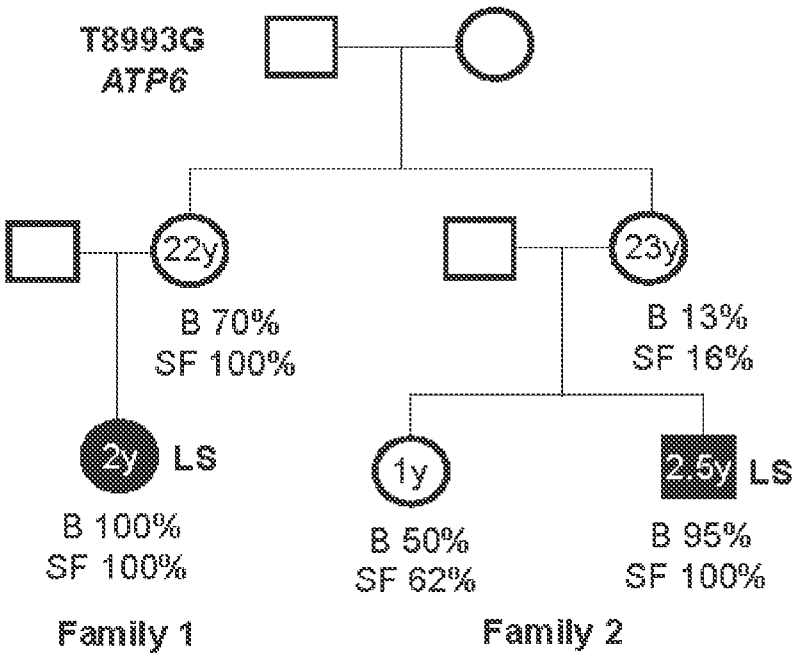


Figure 6B

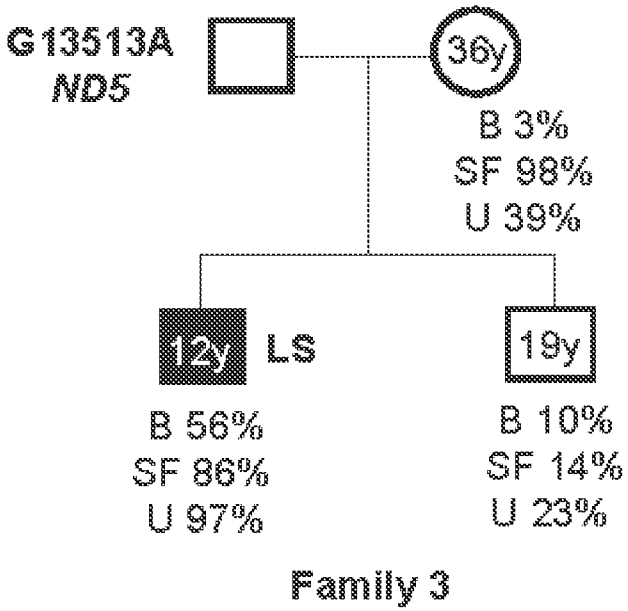


Figure 6C

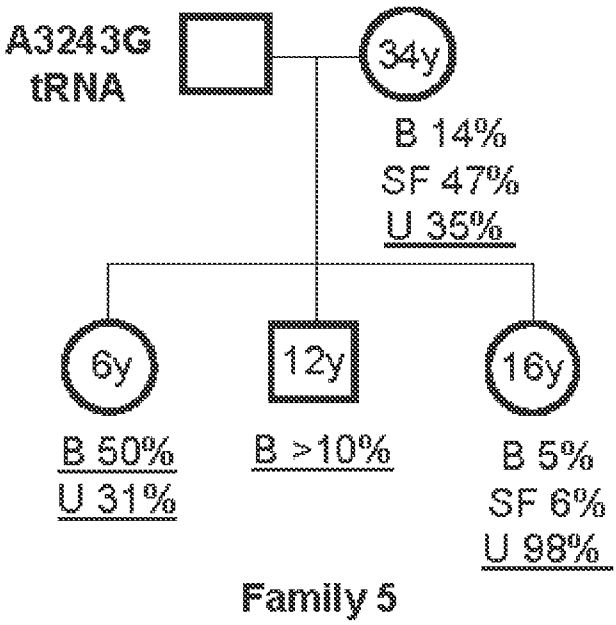


Figure 7A

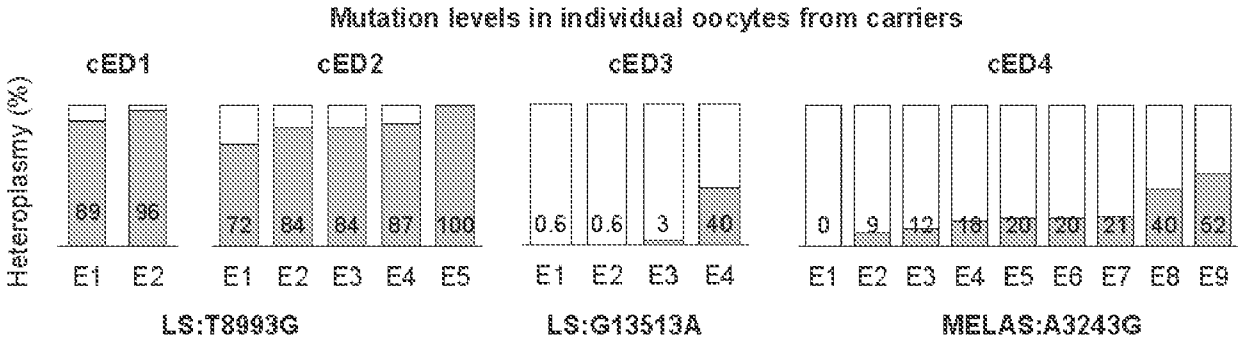


Figure 7B

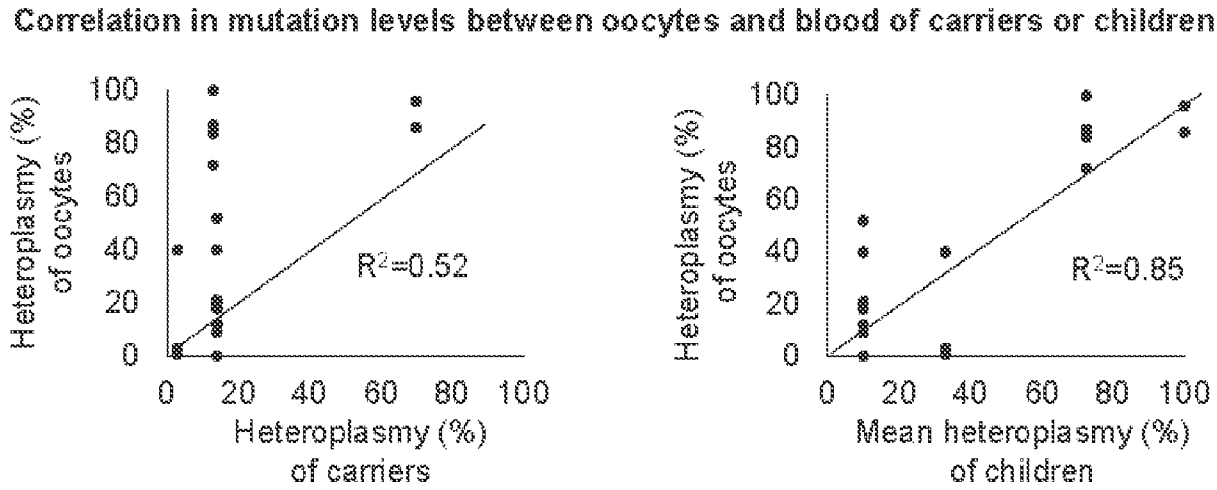


Figure 7C

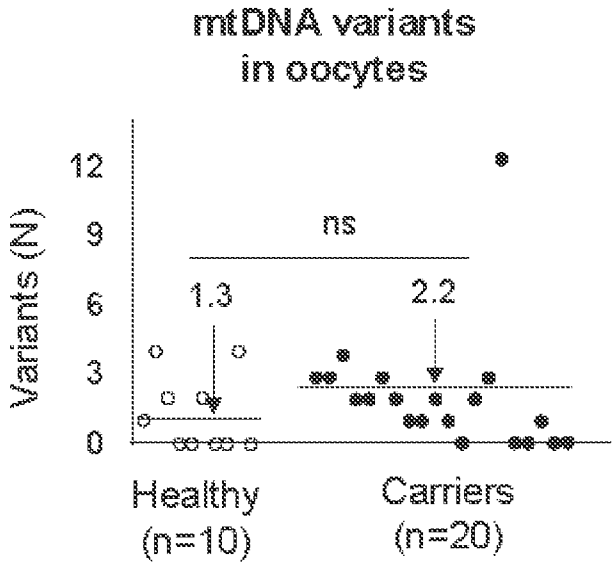


Figure 7D

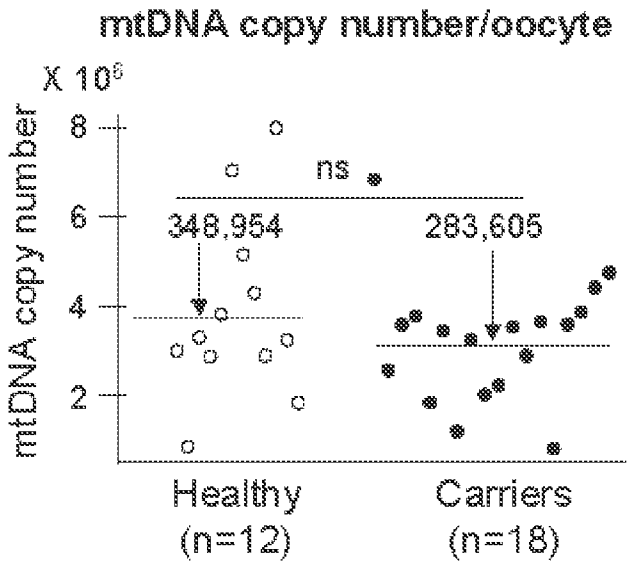


Figure 8A

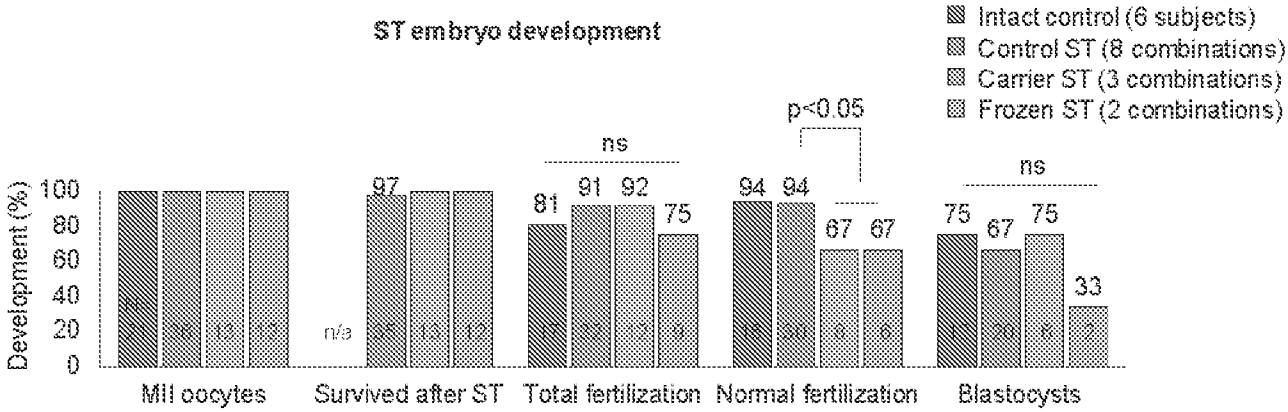


Figure 8B

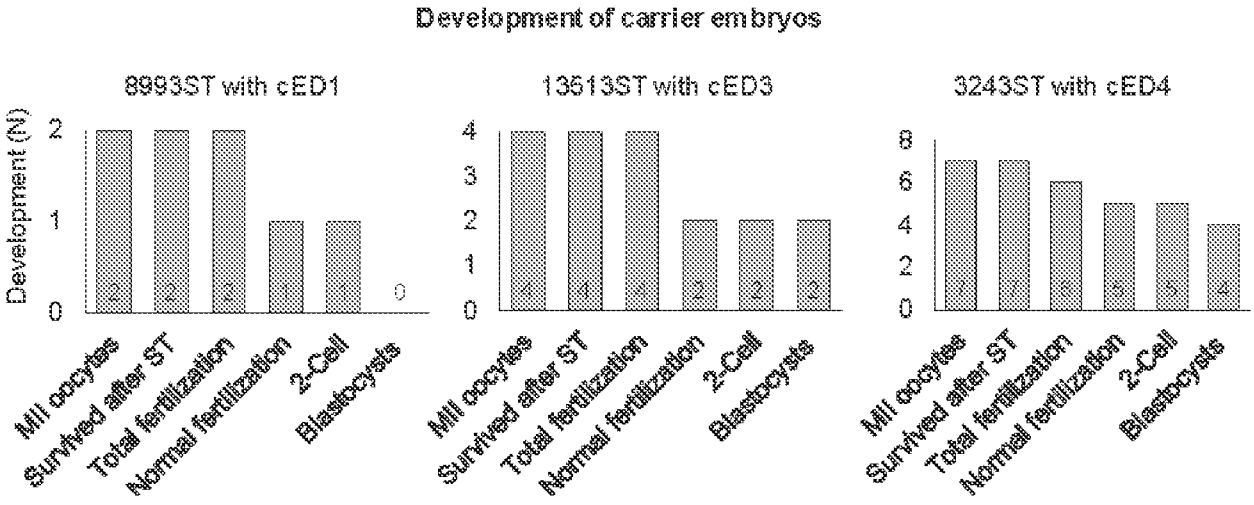


Figure 8C

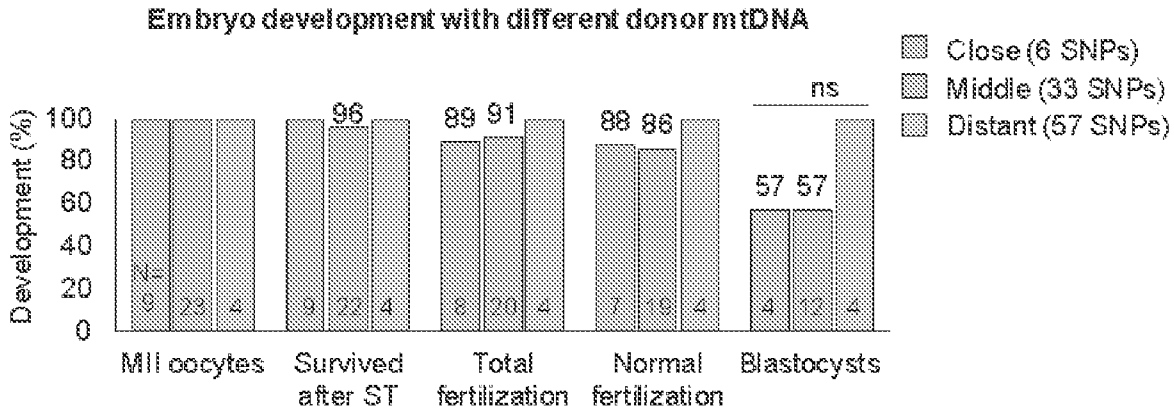


Figure 8D

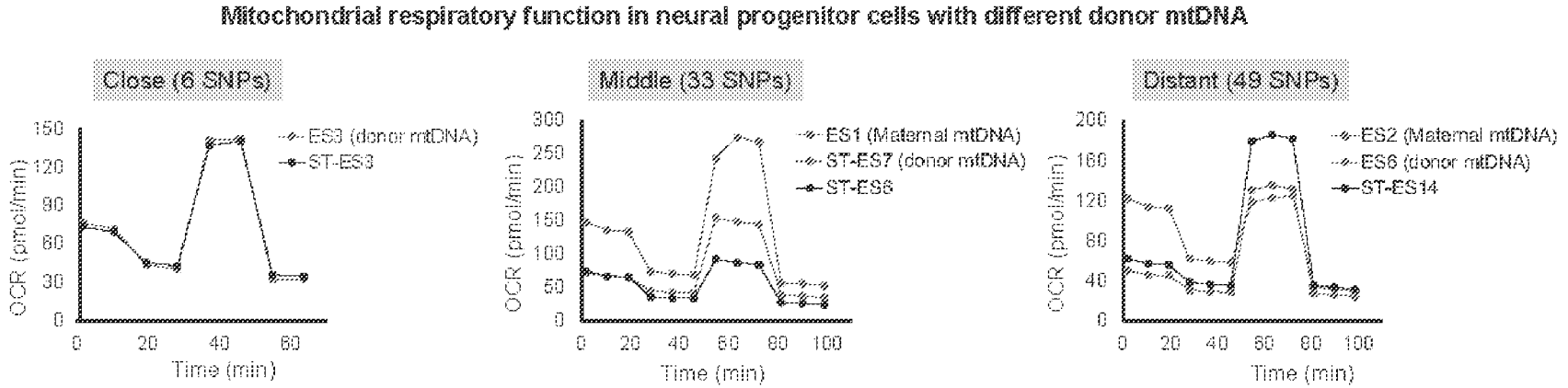


Figure 9A

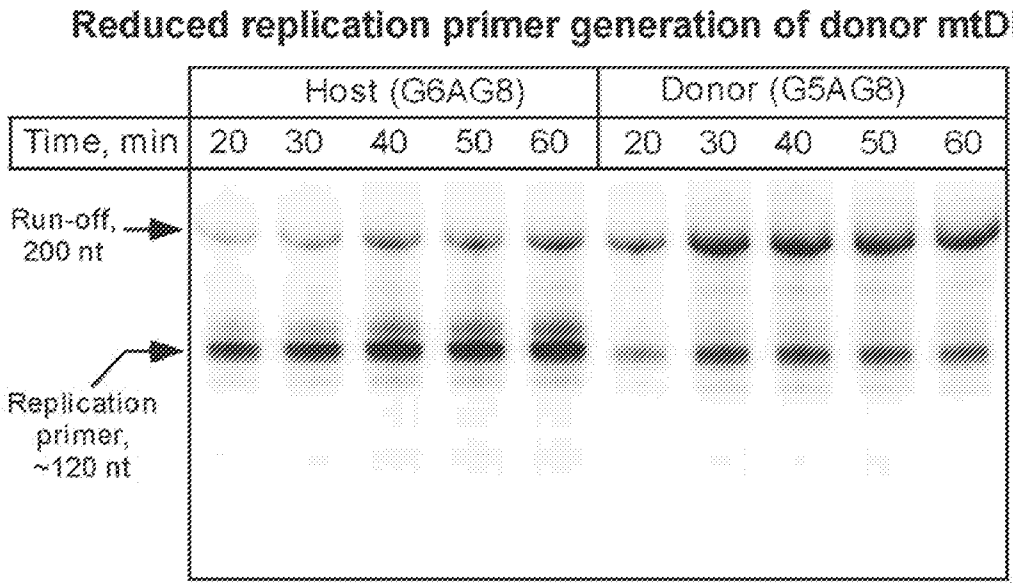


Figure 9B

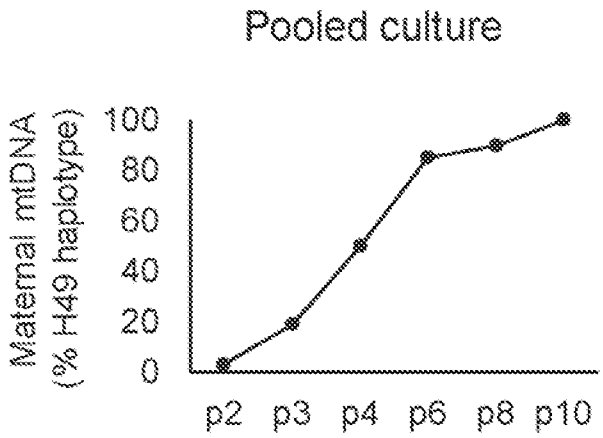


Figure 9C

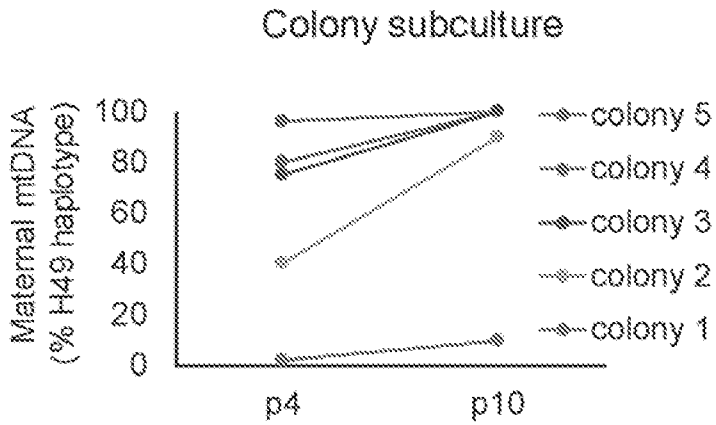


Figure 9D

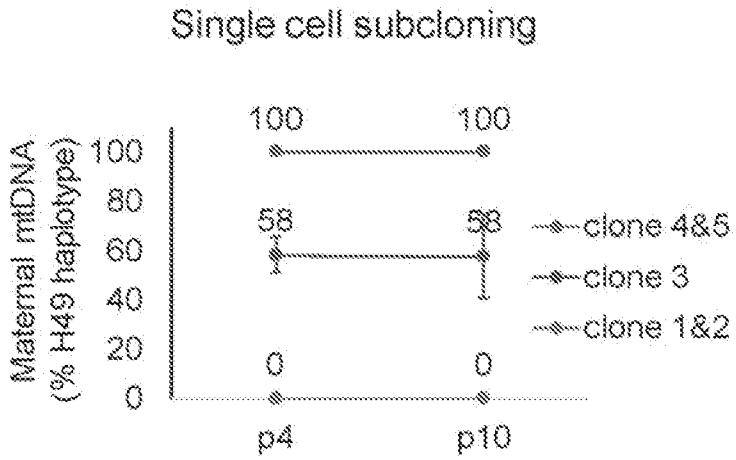
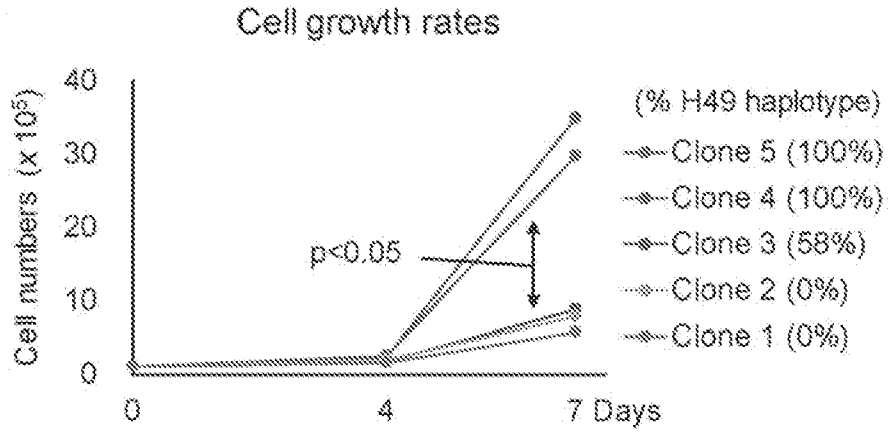


Figure 9E


Cell growth rates
Cell numbers (x 10^5)
40
30
20
10
0
0
4
7 Days
p<0.05
(% H49 haplotype)
Clone 5 (100%)
Clone 4 (100%)
Clone 3 (58%)
Clone 2 (0%)
Clone 1 (0%)

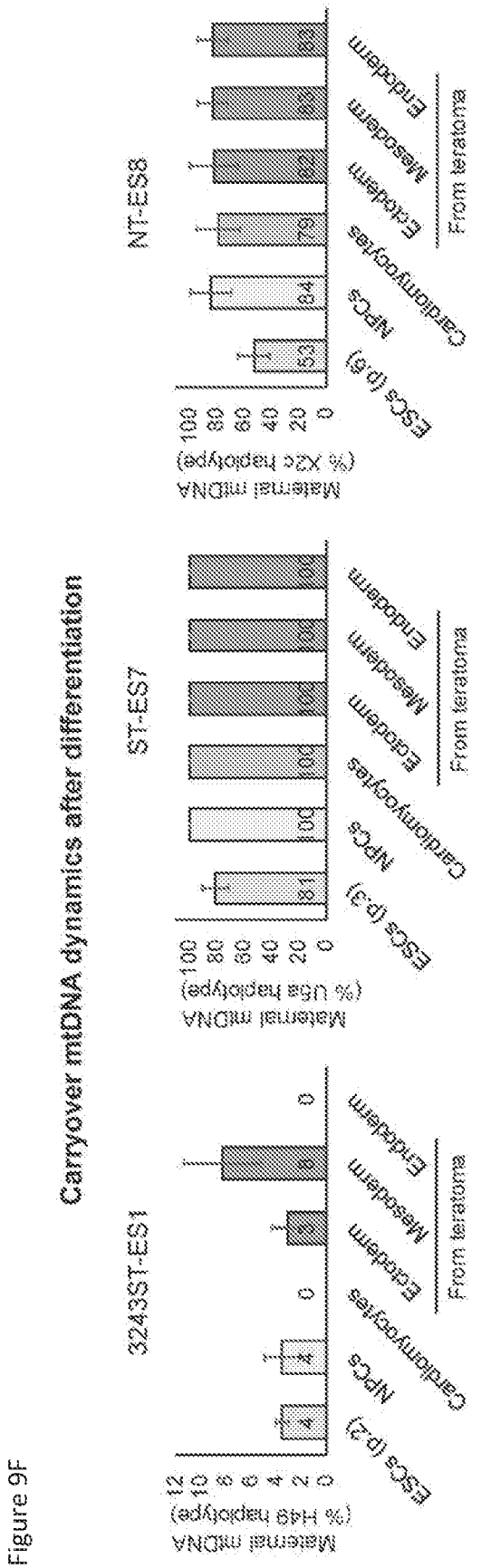

Carryover mtDNA dynamics after differentiation
3243ST-ES1
ST-ES7
NT-ES8
Maternal mtDNA (% H49 haplotype)
Maternal mtDNA (% U5a haplotype)
Maternal mtDNA (% X2c haplotype)
ESCs (p.2)
NPCs
Cardiomyocytes
Ectoderm
Mesoderm
Endoderm
From teratoma

Figure 9F

Figure 10A

Information on families with mitochondrial disease

Mitochondria disease	Family	Affected member	Age (yr)	Clinical manifestation	Mother's age (yr)	mtDNA mutation	Gene
Leigh syndrome	F1	Daughter	2	Seizures, metabolic acidosis, developmental delay, difficulty to thrive, abnormal basal ganglia and enlargement heart ventricle	22	T8993G	*ATP6* (non-syn)
	F2	Son	2.5	Seizures, chronic acidosis, developmental delay, difficulty to thrive and encephalopathy	23	T8993G	*ATP6* (non-syn)
	F3	Son	12	Seizures, failure to thrive, difficulty in breathing, enlarged heart ventricle, kidney failure and optic nerve atrophy	36	G13513A	*ND5* (non-syn)
	F4	Daughter	1	Seizures, difficulty to thrive, lactic acidosis, neuro-motor impairment and history of congenital brain abnormality	28	No	n/a
MELAS syndrome	F5	Maternal sister	23	Mitochondrial encephalomyopathy, lactic acidosis and stroke-like episodes	32	A3243G	tRNA (Leucine)

Figure 10B

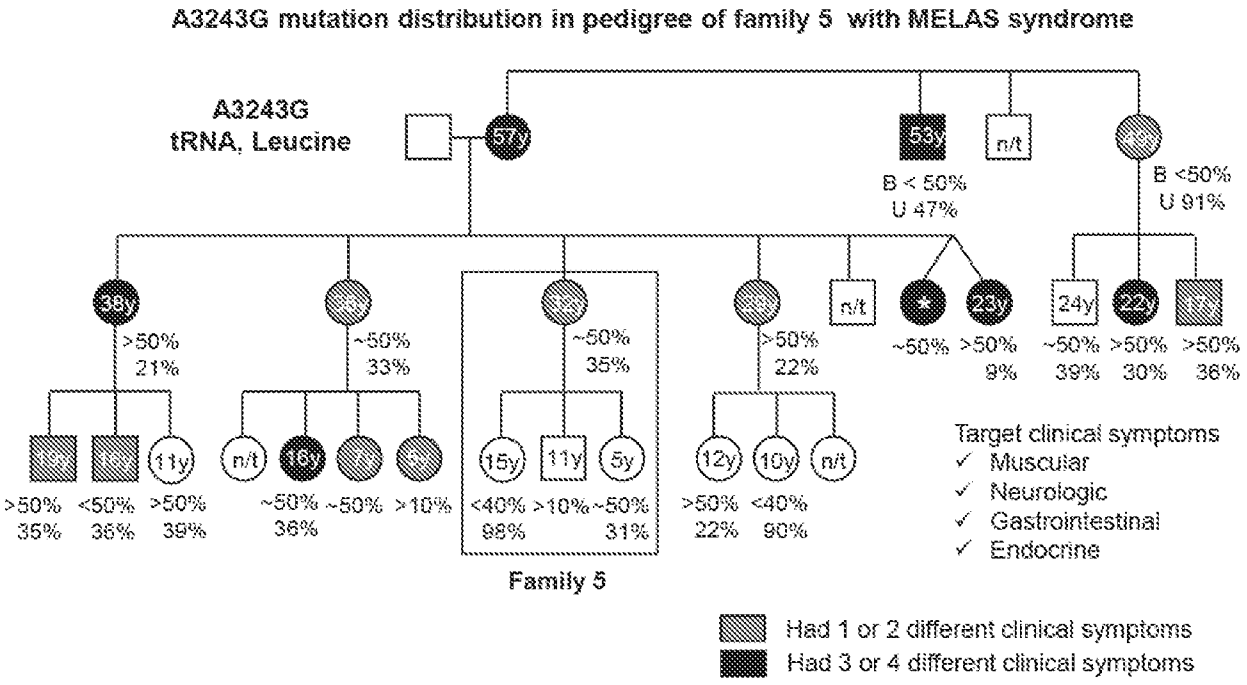


Figure 11A

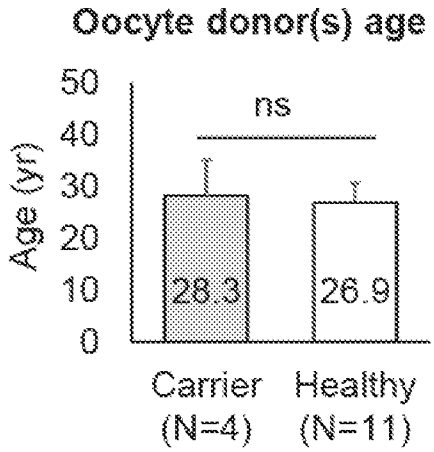


Figure 11B

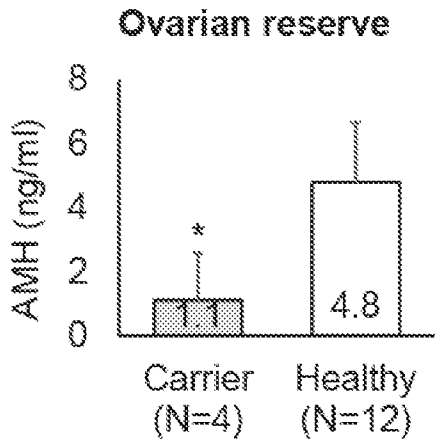


Figure 11C

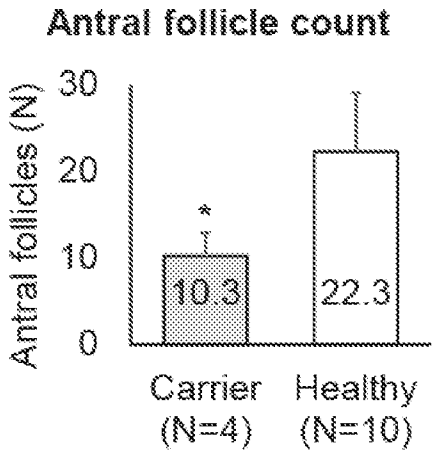


Figure 11D

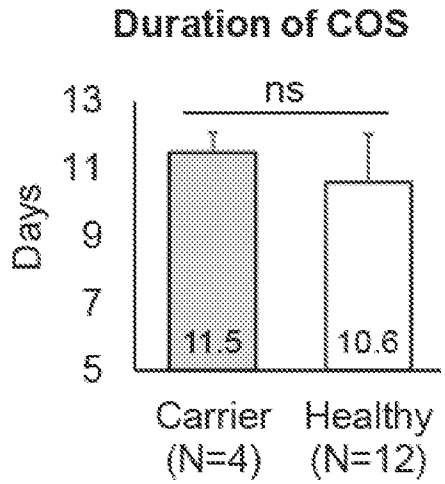


Figure 11E

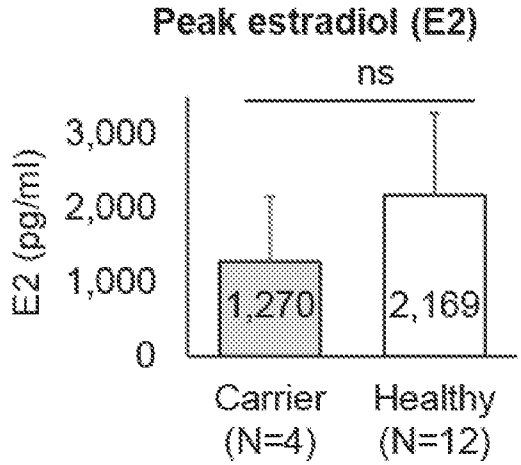


Figure 11F

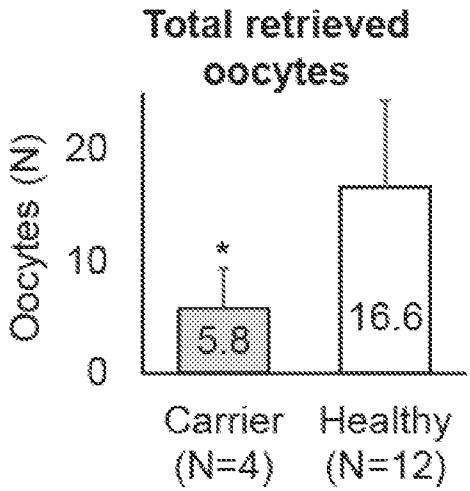


Figure 11G

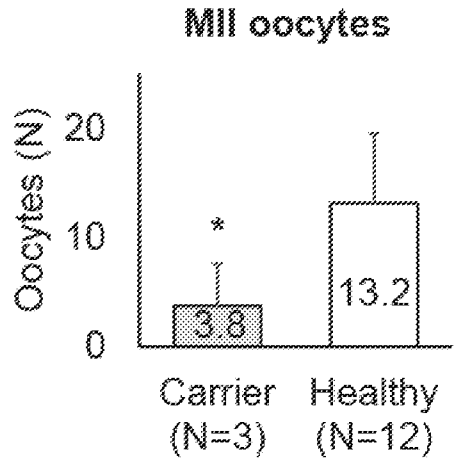


Figure 11H

Responses to controlled ovarian stimulation in women carrying pathogenic mtDNA mutations

Oocyte donor	Family	Age (yr)	Duration of birth control (yr)	BMI (kg/m^2)	AMH (ng/ml)	AFC (N)	Peak E2 (pg/ml)	Duration of Stimulation (days)	Retrieved Oocytes (N)	Mature MII oocytes (N)
cED1	F1	22	2	22.1	0.2	9	280	11	3	2
cED2	F2	23	none	34.1	3.3	10	797	11	5 (premature luteinization)	n/a
cED3	F3	36	12	23.5	0.5	8	1848	12	4	4
cED4	F5	32	none	33.1	0.4	14	2156	12	11	9

Figure 11I

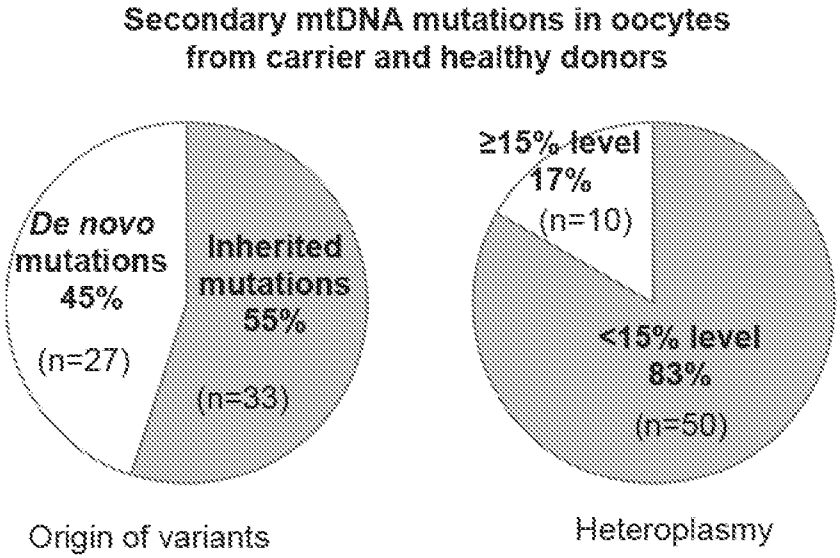


Figure 11J

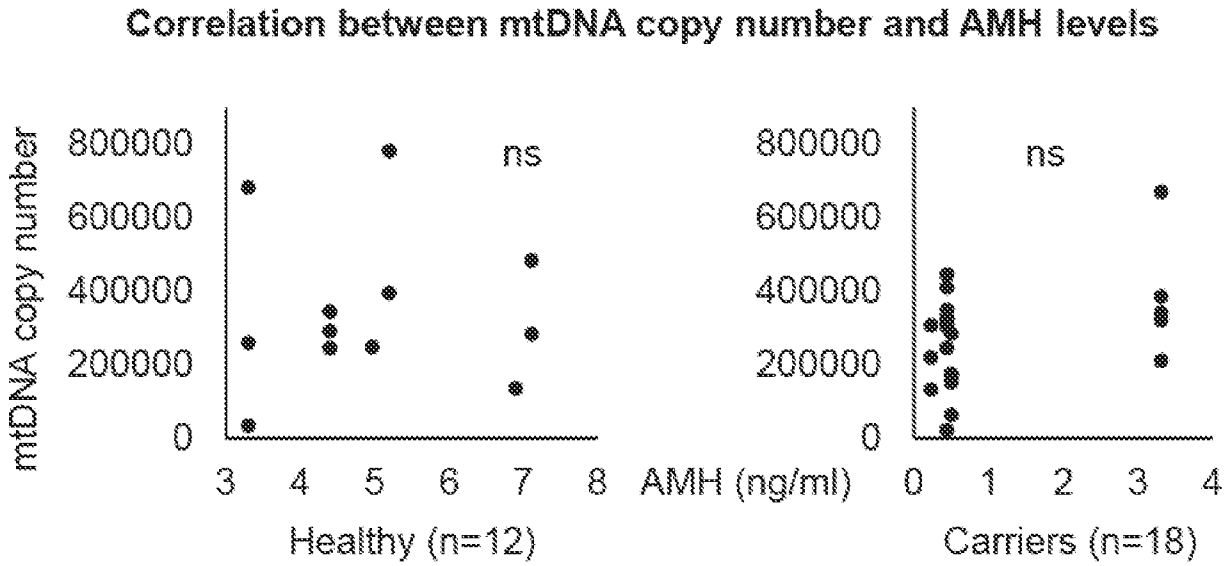


Figure 12A

Donor oocyte mtDNA haplotypes and SNP differences in ST embryos

Cyto / Karyo	Egg donor	hED1 (21-yr)	hED2 (29-yr)	hED3 (23-yr)	hED4 (25-yr)	hED5 (25-yr)	hED6 (28-yr)	hED7 (24-yr)	hED8 (34-yr)	hED9 (32-yr)	hED10 (27-yr)	hED11 (29-yr)
Egg donor	mtDNA haplotype	L2c	D4a	A2g	B2k	U5a	V3	T2	H1b	H2a	H6a	H56
hED1 (21-yr)	L2c									57		
hED2 (29-yr)	D4a			49								
hED3 (23-yr)	A2g		49									
hED5 (25-yr)	U5a						33		33			
hED6 (28-yr)	V3					33						
hED8 (34-yr)	H1b					33						
hED9 (32-yr)	H2a	57										6
hED11 (29-yr)	H56									6		
cED1 (22-yr)	H1b										20	
cED3 (36-yr)	T2b							22				
cED4 (32-yr)	H49				32							

Figure 12B

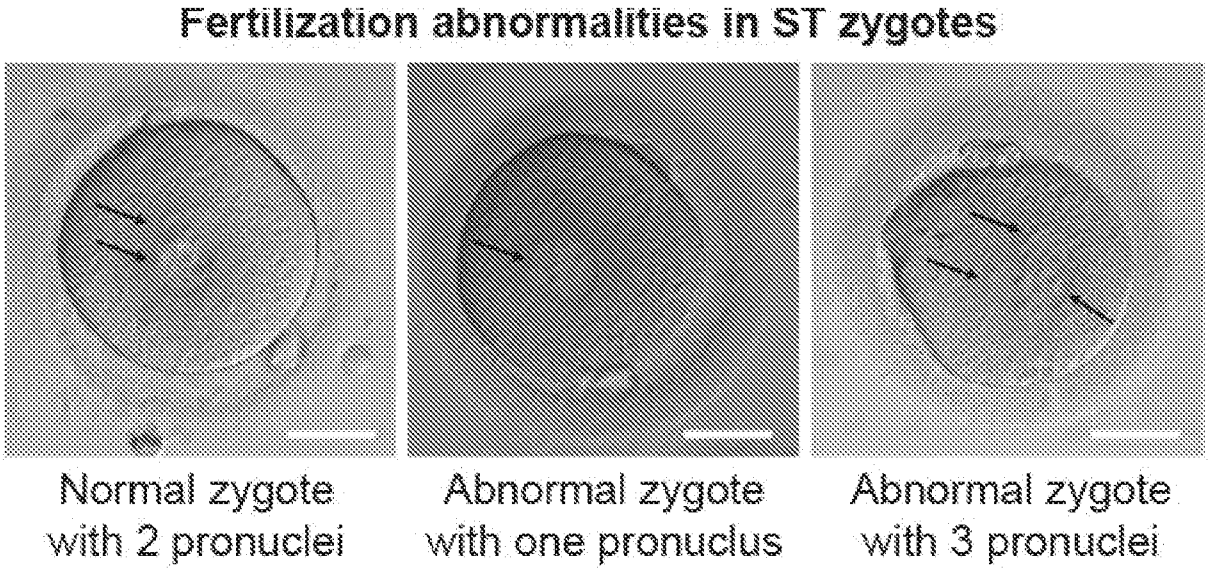


Figure 12C

Fertilization abnormalities in ST zygotes and embryos

Treatment	Total fertilized zygotes (N)	Total abnormal fertilized zygotes (%)	Abnormal No. of pronuclei			Blastocysts	Karyotypes
			One	Three (%)	Abnormal divided		
Intact control	17	1 (6)	1	0	0	0	
Control ST	32	2 (6)	1		0	0	
				1 (3)		1	69,XXY
Carrier ST	12	4 (33)	1	2 (17)	1	0	

Figure 12D

Fertilization and embryo development of frozen ST oocytes

Treatment	MII oocytes (N)	Survived after ST (%)	Total fertilization (%)	Normal fertilization (%)	Abnormal N. pronuclei		Normal morale (%)	Normal blastocysts (%)
					One	Three (%)		
Vitrified cytoplasts/ Fresh spindles	6	6 (100)	6 (100)	4 (67)	1	1 (17)	4 (100)	1 (25)
Vitrified spindles/ Fresh cytoplasts	6	6 (100)	3 (50)	2 (67)	0	1 (33)	2 (100)	1 (50)

Figure 12E

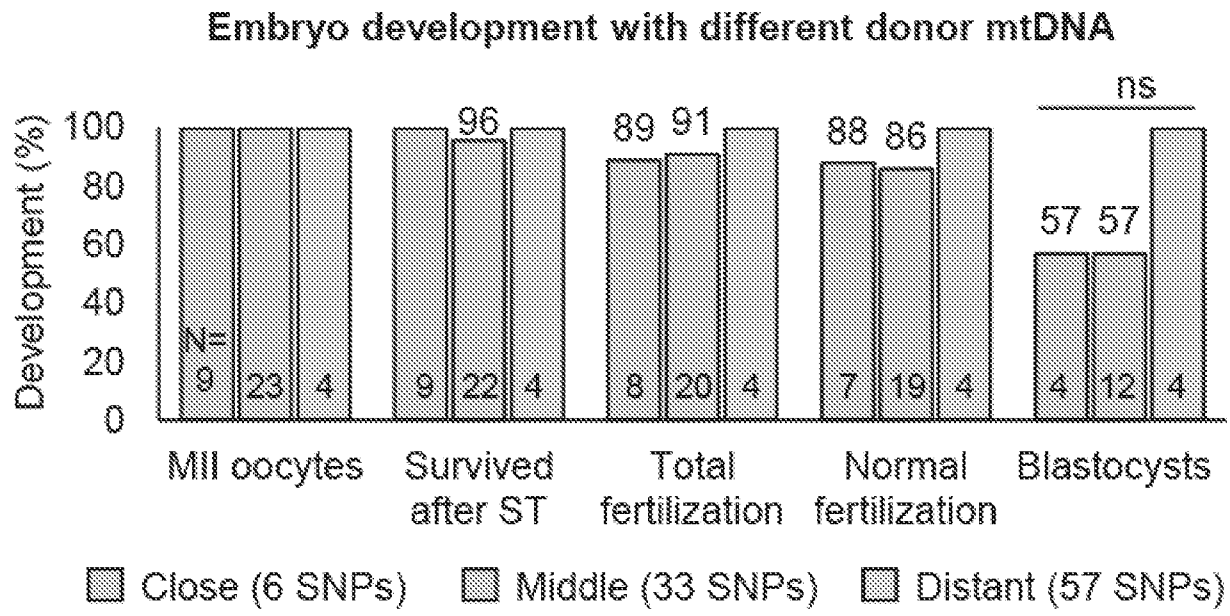


Figure 13A

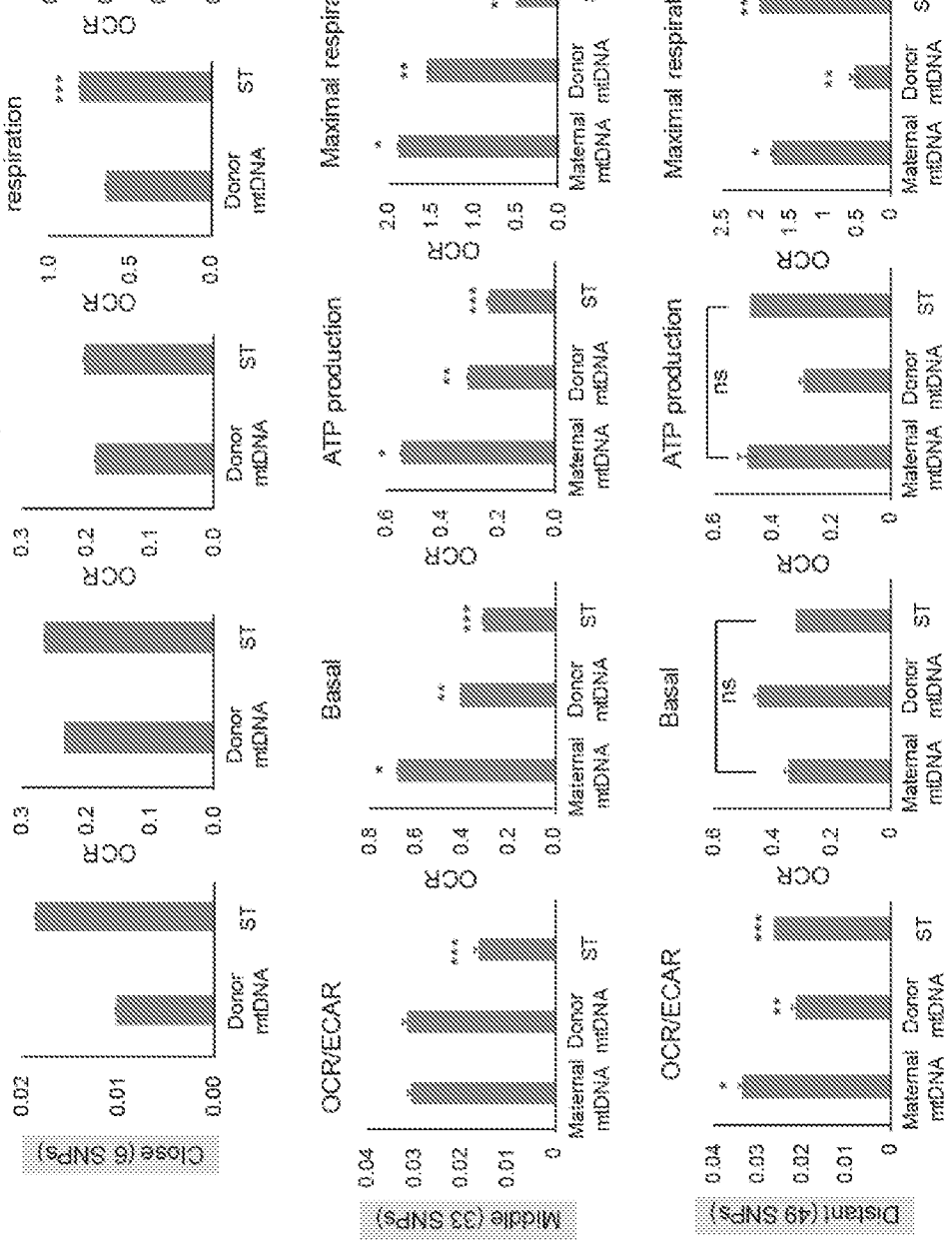

Mitochandrial respiratory function in neural progenitor cells with different donor mtDNA
OCR/ECAR
Basal
ATP production
Maximal respiration
Spare respiratory capacity
Close (6 SNPs)
Middle (33 SNPs)
Distant (49 SNPs)
OCR
Maternal mtDNA
Donor mtDNA
ST
ns

Figure 13B

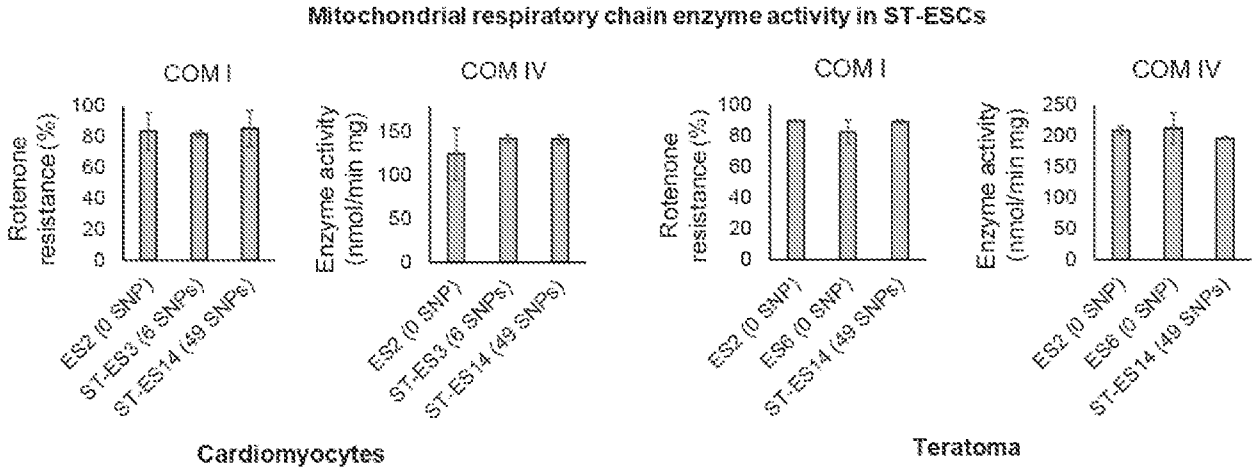


Figure 14A

***In vivo* and *in vitro* differentiation of MRT-ESCs**

No.	Cell line	Maternal mtDNA haplotype	Donor mtDNA haplotype (s)	SNP difference	Teratoma	NPCs	Cardiomyocytes
1	ES1	---------- H1b control ----------		0	nt	yes	yes
2	ES2	---------- D4a control ----------		0	yes	yes	yes
3	ES3	---------- H56 control ----------		0	nt	yes	yes
4	ES6	---------- A2g control ----------		0	yes	yes	yes
5	ST-ES3	H2a	H56	6	nt	yes	yes
6	ST-ES6	H1b	U5a	33	nt	yes	yes
7	ST-ES7	U5a	H1b/ U5a (reversed)	33	nt	yes	yes
8	ST-ES14	D4a	A2g	49	yes	yes	yes
9	ST3243-ES1	H49	B2k/ H49 (reversed)	31	yes	yes	yes
10	ST3243-ES2	H49	B2k	31	yes	yes	yes
11	NT-ES8	X2c	D4a/ X2c (reversed)	39	yes	yes	yes

Figure 14B

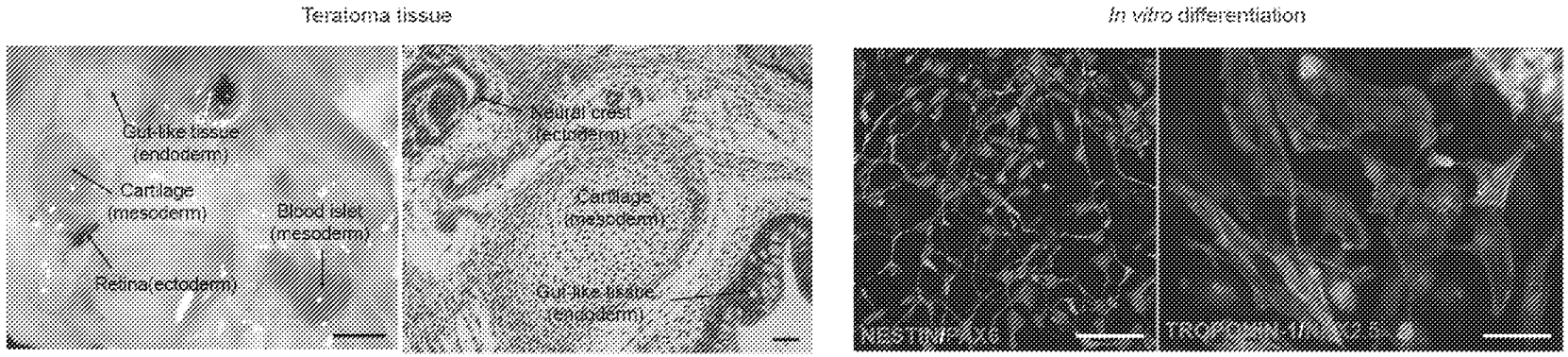
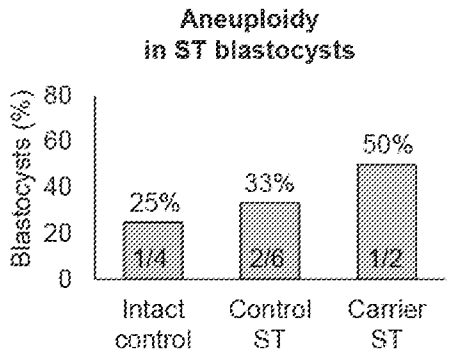


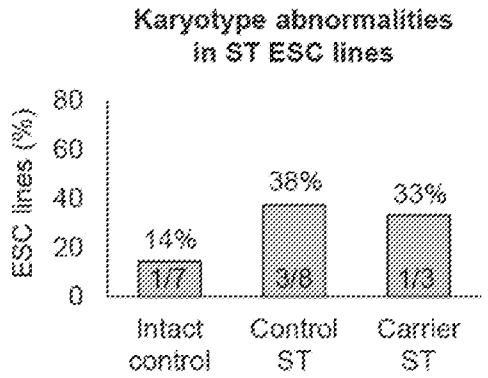
Figure 15A



Summary of array CGH in intact and ST blastocysts

Treatment	#	Age of nuclear donor (yr)	Egg donor ID	aCGH Results	Sex
Intact control	1	34	hED8	Abnormal: -21	Male
	2	29	hED11	Normal	Male
	3	25	hED4	Normal	Female
	4	25	hED4	Normal	Male
Control ST	1	34	hED8	Abnormal: +7, +15	Male
	2	32	hED9	Normal	Male
	3	32	hED9	Normal	Female
	4	32	hED9	Normal	Male
	5	29	hED11	Abnormal: +12	Male
	6	21	hED1	Normal	Male
Carrier ST	1	36	cED3	Abnormal:+9	Male
	2	32	cED4	Normal	Female

Figure 15B



G-banding analysis of ESC lines derived from intact and ST blastocysts

Treatment	#	Age of nuclear donor (yr)	Egg donor ID	ESC line	Karyotype
Intact control	1	34	hED8	ES1	46,XX
	2	29	hED2	ES2	46,XX
	3	29	hED11	ES3	46,XY
	4	25	hED4	ES4	46,XY
	5	25	hED5	ES5	46,XX
	6	23	hED3	ES6	46,XX
	7	23	hED3	ES7	45,XY,-21
Control ST	1	34	hED8	ST-ES5	Mosaicism 47,XX +10 [12]/46,XX [8]
	2	34	hED8	ST-ES6	46,XX
	3	32	hED9	ST-ES3	46,XX
	4	29	hED2	ST-ES14	46,XY
	5	28	hED6	ST-ES10	45,X
	6	25	hED5	ST-ES7	46,XY
	7	25	hED5	ST-ES8	92,XXXX
	8	25	hED5	ST-ES9	46,XY
Carrier ST	1	36	cED3	13513 ST-ES	47,XY,+9
	2	32	cED4	3243 ST-ES1	46,XX
	3	32	cED4	3243 ST-ES2	46,XY

Figure 16A

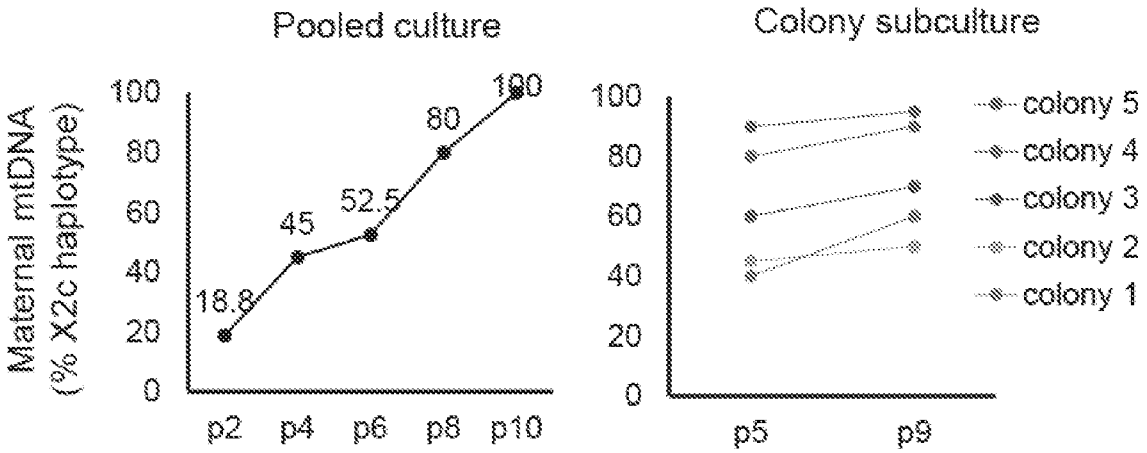


Figure 16B

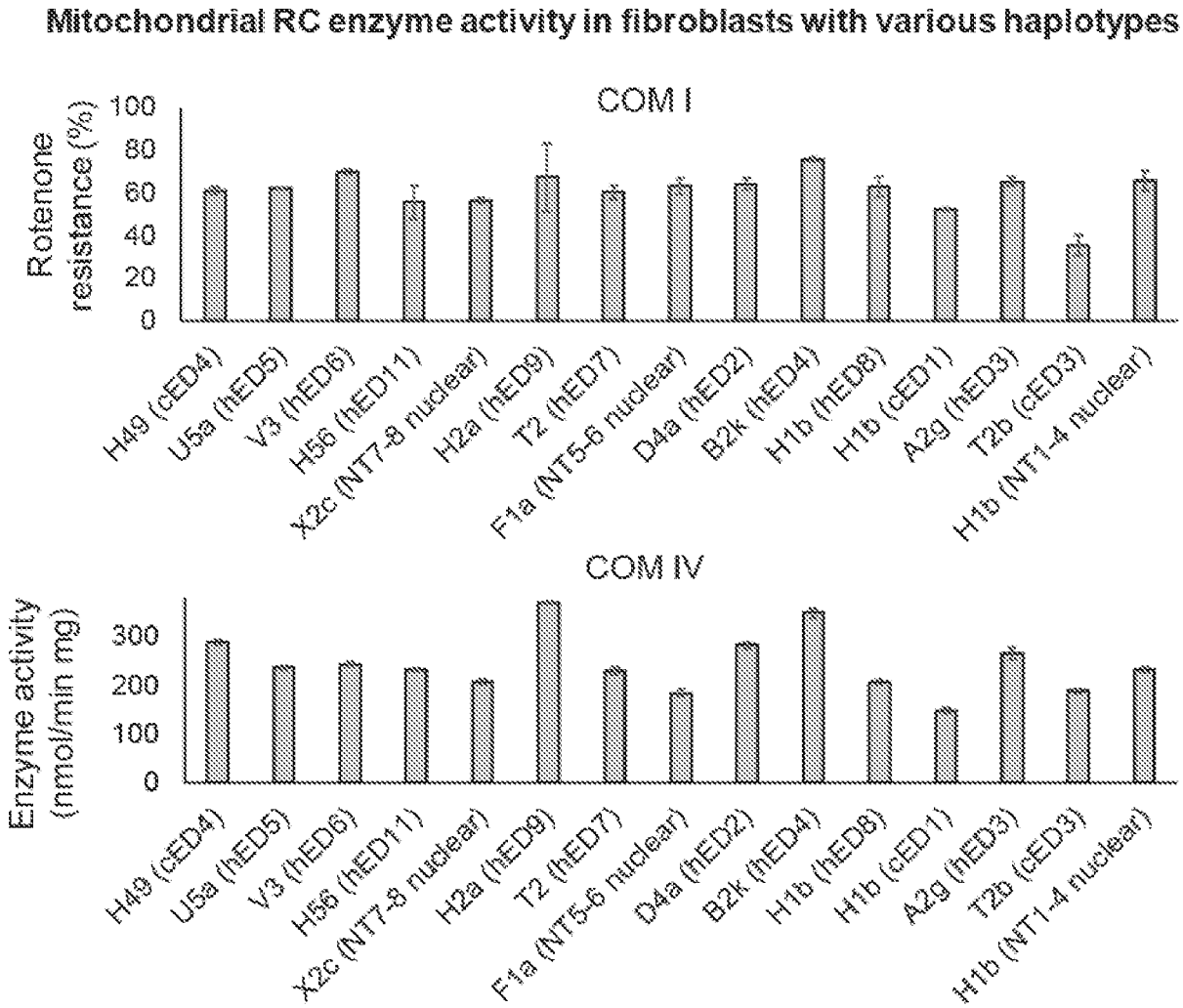


Figure 17

Treatment	#	ESC line ID	CNVs	Chromosome Location	CNV chromosome	Interpretation
Intact control	1	ES1	Deletion (neutral)	15q11.2	male	699 kb region of chromosome 15 (15q11.2) shows low level mosaicism (approximately 10%-20%) for homozygosity of uncertain clinical significance.
	2	ES5	Deletion (neutral)	15q11.2	male	1.1 Mb region of chromosome 15 (15q11.2) shows mosaicism for homozygosity of uncertain clinical significance.
			Deletion (neutral)	Xp22.33-q28	male	Less than 10% of cells of the entire chromosome X (Xp22.33-Xq28) of uncertain clinical significance.
Control ST	1	ST-ES5	Duplication	10p15.3-q26.3	male	Mosaic trisomy 10.
			Deletion (neutral)	15q11.2	male	549 kb region of chromosome 15 (15q11.2) shows mosaicism for homozygosity of uncertain clinical significance.
			Deletion	Xp22.33-q28	male	Monosomy X (Xp22.33-Xq28) of uncertain clinical significance.
	2	ST-ES6	None	n/a		n/a
	3	ST-ES7	None	n/a		n/a
	4	ST-ES9	None	n/a		n/a
Carrier ST	1	3243ST-ES1	None	n/a		n/a
	2	3243ST-ES2	Deletion (neutral)	15q11.2	male	791 kb region of chromosome 15 (15q11.2) shows mosaicism for homozygosity of uncertain clinical significance.

Figure 18

	Family 1	Family 2	Family 3		Family 4	Family 5			
Mitochondrial disease	LS	LS	LS		LS	MELAS			
Pathogenic mtDNA mutation	T8993G	T8993G	G13513A		No	A3243G			
Age of carrier (yr)	22	23	36		28	32			
COS	Yes	Yes	Yes		Excluded	Yes			
No. retrieved oocytes	3	5	4		n/a	11			
No. ST oocytes	2	Canceled	4		n/a	7			
ST blastocysts	0	n/a	2		n/a	4			
Grade at D6	n/a	n/a	5AA	5BB	n/a	5AA	5AA	5BB	5CC
Aneuploidy	n/a	n/a	Yes:+9	n/t	n/a	n/t	No	No	No
Sex	n/a	n/a	M	n/a	n/a	n/a	M	F	F
mtDNA carryover	n/a	n/a	< 1%	n/a	n/a	n/a	< 1%	< 1%	< 1%*

INTERNATIONAL SEARCH REPORT

International application No.
PCT/US2017/060720

A. CLASSIFICATION OF SUBJECT MATTER

IPC(8) - C12N 5/00; C12N 5/02; C12N 5/073; C12N 5/0735; C12N 5/075; C12N 5/16 (2018.01)
CPC - A61K 35/54; C12N 7/00; C12N 2500/44; C12N 2500/84; C12N 2517/04 (2018.02)

According to International Patent Classification (IPC) or to both national classification and IPC

B. FIELDS SEARCHED

Minimum documentation searched (classification system followed by classification symbols)
See Search History document

Documentation searched other than minimum documentation to the extent that such documents are included in the fields searched
USPC - 424/9.321; 435/44; 435/455 (keyword delimited)

Electronic data base consulted during the international search (name of data base and, where practicable, search terms used)
See Search History document

C. DOCUMENTS CONSIDERED TO BE RELEVANT

Category*	Citation of document, with indication, where appropriate, of the relevant passages	Relevant to claim No.
X -- Y	US 6,143,564 A (WAKAYAMA et al) 07 November 2000 (07.11.2000) entire document	1-3, 10 --- 4, 5
Y	US 2014/0335619 A1 (MITALIPOV et al) 13 November 2014 (13.11.2014) entire document	4, 5, 9
Y	US 2014/0308257 A1 (NEW YORK STEM CELL FOUNDATION) 16 October 2014 (16.10.2014) entire document	6-9, 14-17
Y	TSAI et al. "The Relationship Between Mitochondrial DNA Haplotype and the Reproductive Capacity of Domestic Pigs (Sus scrofa domesticus)," BMC Genetics, 18 May 2016 (18.05.2016), Vol. 17, No. 67, Pgs. 1-17. entire document	6-9
Y	LI et al. "Physiology and Pathophysiology of Mitochondrial DNA," Advances in Experimental Medicine and Biology, 08 January 2016 (08.01.2016) Vol. 942, Pgs. 1-17. entire document	14-17
P, X	MA et al. "Functional Human Oocytes Generated by Transfer of Polar Body Genomes," Cell Stem Cell, 05 January 2017 (05.01.2017), Vol. 20, Iss. 1, Pgs. 112-119. entire document	1-10, 14-17
P, A	KANG et al. "Mitochondrial Replacement in Human Oocytes Carrying Pathogenic Mitochondrial DNA Mutations," Nature, 08 December 2016 (08.12.2016), Vol. 540, No. 7632, Pgs. 270-275. entire document	1-10, 14-17

☐ Further documents are listed in the continuation of Box C. ☐ See patent family annex.

* Special categories of cited documents:
"A" document defining the general state of the art which is not considered to be of particular relevance
"E" earlier application or patent but published on or after the international filing date
"L" document which may throw doubts on priority claim(s) or which is cited to establish the publication date of another citation or other special reason (as specified)
"O" document referring to an oral disclosure, use, exhibition or other means
"P" document published prior to the international filing date but later than the priority date claimed
"T" later document published after the international filing date or priority date and not in conflict with the application but cited to understand the principle or theory underlying the invention
"X" document of particular relevance; the claimed invention cannot be considered novel or cannot be considered to involve an inventive step when the document is taken alone
"Y" document of particular relevance; the claimed invention cannot be considered to involve an inventive step when the document is combined with one or more other such documents, such combination being obvious to a person skilled in the art
"&" document member of the same patent family

Date of the actual completion of the international search	Date of mailing of the international search report
27 February 2018	26 MAR 2018
Name and mailing address of the ISA/US Mail Stop PCT, Attn: ISA/US, Commissioner for Patents P.O. Box 1450, Alexandria, VA 22313-1450 Facsimile No. 571-273-8300	Authorized officer Blaine R. Copenheaver PCT Helpdesk: 571-272-4300 PCT OSP: 571-272-7774

INTERNATIONAL SEARCH REPORT

International application No.
PCT/US2017/060720

Box No. II Observations where certain claims were found unsearchable (Continuation of item 2 of first sheet)

This international search report has not been established in respect of certain claims under Article 17(2)(a) for the following reasons:

1. ☐ Claims Nos.:
because they relate to subject matter not required to be searched by this Authority, namely:

2. ☐ Claims Nos.:
because they relate to parts of the international application that do not comply with the prescribed requirements to such an extent that no meaningful international search can be carried out, specifically:

3. ☒ Claims Nos.: 11-13
because they are dependent claims and are not drafted in accordance with the second and third sentences of Rule 6.4(a).

Box No. III Observations where unity of invention is lacking (Continuation of item 3 of first sheet)

This International Searching Authority found multiple inventions in this international application, as follows:

1. ☐ As all required additional search fees were timely paid by the applicant, this international search report covers all searchable claims.

2. ☐ As all searchable claims could be searched without effort justifying additional fees, this Authority did not invite payment of additional fees.

3. ☐ As only some of the required additional search fees were timely paid by the applicant, this international search report covers only those claims for which fees were paid, specifically claims Nos.:

4. ☐ No required additional search fees were timely paid by the applicant. Consequently, this international search report is restricted to the invention first mentioned in the claims; it is covered by claims Nos.:

Remark on Protest

☐ The additional search fees were accompanied by the applicant's protest and, where applicable, the payment of a protest fee.

☐ The additional search fees were accompanied by the applicant's protest but the applicable protest fee was not paid within the time limit specified in the invitation.

☐ No protest accompanied the payment of additional search fees.